Cuadernos de Investigación Geográfica *Geographical Research Letters*	2024	Nº 50 (1)	pp. 145-178	EISSN 1697-9540

http://doi.org/10.18172/cig.5739

ANALYSIS OF PLANT PHENOLOGY DYNAMICS IN SPAIN FROM 1983 TO 2020 USING SATELLITE IMAGERY

MARIA ADELL-MICHAVILA[1,2]*, SERGIO M. VICENTE-SERRANO[3], RAQUEL MONTORIO-LLOVERIA[1,2], ZANGZANG CAI[4], LARS EKLUNDH[4]

[1]*Departamento de Geografía y Ordenación del Territorio, Universidad de Zaragoza, Spain.*

[2]*Grupo GEOFOREST-IUCA, Universidad de Zaragoza, Spain.*

[3]*Instituto Pirenaico de Ecología, Consejo Superior de Investigaciones Científicas, Spain.*

[4]*Department of Geography, Lund University, Lund, Sweden.*

ABSTRACT. This study spatially analyzes plant phenology and its variations over time in mainland Spain and the Balearic Islands. To conduct the analysis, a nearly 40-year span time series (1983-2020) was generated by merging NDVI vegetation index values from satellite images sourced from NOAA-AVHRR and MODIS sensors. The phenological variables were calculated using TIMESAT 3.3, which extracted 13 phenometrics whose trends were evaluated using the Theil-Sen model, and their significance was assessed with the Mann-Kendall test. The results reveal regional differences between Eurosiberian Spain and the Mediterranean region regarding the start and end phases of the season. On average, the Eurosiberian zones have experienced delays in their season start and end dates, by approximately 0.35 and 0.22 days per year over the study period, respectively, while the Mediterranean region has seen an advancement in leaf-out and senescence dates by about 0.07 and 0.05 days per year. A greening trend across the entire study area and significant contrasts among land covers have also been observed, opening avenues for future studies to delve deeper into these behavioral differences and their interactions with changes in climate and land management.

Evaluación espacialmente continua de la dinámica de la fenología vegetal en España entre 1983 y 2020 a partir de imágenes de satélite

RESUMEN. En este estudio se analiza espacialmente la fenología vegetal y sus variaciones a lo largo del tiempo en la España peninsular e Islas Baleares. Para realizar el análisis se ha generado una serie temporal de casi 40 años (1983-2020) a partir de la fusión de valores del índice de vegetación NDVI de imágenes de satélite procedentes de los sensores NOAA-AVHRR y MODIS. El cálculo de las variables fenológicas se ha realizado con TIMESAT 3.3. que ha extraído 13 fenométricas cuya tendencia se ha evaluado a partir del modelo Theil-Sen y la significación de esta con el test de Mann Kendal. Los resultados muestran diferencias regionales entre la España eurosiberiana y la mediterránea respecto a las fenofases de inicio y final de temporada. Las zonas eurosiberianas de media han visto retrasadas sus fechas de inicio y final de temporada, en torno a 0,35 y 0,22 días cada año a lo largo del periodo de estudio respectivamente, mientras que la región mediterránea ha adelantado las fechas de salida de las hojas y la senescencia de media alrededor de 0,07 y 0,05 días al año. También se ha observado una tendencia al reverdecimiento de toda el área de estudio e importantes contrastes entre las cubiertas del suelo que abren la puerta a futuros estudios que profundicen en estas diferencias de comportamiento y en sus interacciones con los cambios en el clima y en la gestión del territorio.

Keywords: Plant phenology, remote sensing, global change, NOAA-AVHRR, MODIS, NDVI.

Palabras clave: fenología vegetal, teledetección, cambio global, NOAA-AVHRR, MODIS, NDVI.

Received: May 2 2023

Accepted: November 28 2023

***Corresponding author:** Maria Adell-Michavila, Departamento de Geografía y Ordenación del Territorio, Universidad de Zaragoza, España. madell@unizar.es

1. Introduction

Vegetation dynamics are a primary indicator of global change, encapsulating alterations in both the climate system and land use and cover management (Cleland *et al.,* 2007; Menzel, 2002). In this context, various metrics obtained through field observations (e.g., radial growth in trees) (Prislan *et al.*, 2019; Rossi *et al.*, 2011; Rubio-Cuadrado *et al*., 2021) and remote sensing (several vegetation activity or greenness indices) (Motohka *et al.*, 2010; Reed *et al.*, 2009) have been employed to examine vegetation changes due to climate change (Badeck *et al*., 2004; White *et al.*, 2009). Among these methods to measure vegetation dynamics, one of the most robust relates to plant phenology (Bertin, 2008; Cleland *et al.*, 2007), referring to the periodic growth and development cycles of vegetation, typically on an annual scale (Lieth, 1974). From these cycles, several metrics such as the start of growth or the onset of senescence can be derived (Helman, 2018; Reed *et al.*, 2009; Schwartz, 2013), which are recurrent biological processes encompassing various biotic and abiotic causes. Biotic factors influencing vegetation phenology are primarily linked to plant physiology, and the different stages of the phenological cycle are commonly called phenophases. These phenophases are determined by factors such as plant species and development stage, as well as environmental factors like temperature, photoperiod, and availability of water and nutrients, along with their interactions. These factors significantly affect the period during which vegetation is active, easily detectable as this stage usually coincides with the presence of leaves (Lim *et al.*, 2007). Several studies have demonstrated the impact of climate variability and changes on plant phenology (Menzel *et al.*, 2006; Richardson *et al.*, 2013), where the trend towards increasing temperatures has been associated with shifts in key phenological stages, such as the start of the season (leaf unfolding) and the end of the season (color change), leading to an earlier spring, an extension of the vegetative activity period, and a delay in the phenological autumn (Gill *et al.*, 2015; Jeong *et al.*, 2011; Piao *et al.*, 2019).

Plant phenology has multiple ecological implications, as changes therein can alter seasonal interactions among different species (Rathcke and Lacey, 1985; Yang and Rudolf, 2010), with notable consequences for ecosystem biodiversity and productivity (Kharouba *et al.*, 2018). For example, these changes can affect plant-pollinator relationships (Kudo and Ida, 2013), increase vegetative activity, and enhance carbon absorption (Piao *et al.*, 2006; Piao *et al.*, 2019), which in turn have impacts on the ecosystem as a whole. For these reasons, the study of phenology has gained importance, evolving from mere notation of different key moments for vegetation (e.g., the start or end of the season or flowering) to becoming an integral field of experimentation and model generation with broad ecological and climatic significance (Piao *et al.*, 2019; Richardson *et al.*, 2013). In recent decades, there has been a rapid increase in the number of studies focused on plant phenology (Piao *et al.*, 2019), particularly those related to the effects of climate change on vegetation (Menzel *et al.*, 2006; Piao *et al.*, 2019). For instance, both in situ (terrestrial) and satellite measurements have observed a trend of changing phenological patterns in Europe, North America, and East Asia, with an earlier season start over recent decades (Ge *et al.*, 2015; Fu *et al.*, 2014; Wolfe *et al.*, 2005). To a lesser extent, it has also been noted that in Europe, the end of the vegetative period seems to be delayed (Gill *et al.*, 2015).

National and international phenological networks have recorded various parameters of vegetation phenology (Piao *et al.*, 2019). Although there are occasionally very long temporal records (e.g., several centuries for cherry blossom in Japan), the spatial coverage of the records is usually limited (Rodriguez-Galiano *et al.*, 2015) and primarily focused on temperate and subalpine forest areas. Moreover, records are often obtained by different observers and with different methods, without a uniform protocol, making it difficult to integrate and exchange this type of information between different regions (Piao *et al.*, 2019). In Spain, although there is a national phenological observation network maintained by the Spanish Meteorological Agency (AEMET) (MITECO, n.d.), the records are very short and scarce, except in a few locations (García-Mozo *et al.*, 2010; Oteros *et al.*, 2015). For these reasons, in recent decades, numerous research efforts have been made to analyze plant phenology and its changes using data provided by Earth observation satellites. This approach offers an advantageous way to study these terrestrial vegetation cycles due to the existence of continuous and systematic global information.

For these types of studies, images from the AVHRR (Advanced Very High Resolution Radiometer) sensors aboard NOAA (National Oceanic and Atmospheric Administration) satellites, with information since 1981 (Caparros-Santiago and Rodríguez-Galiano 2020; Piao *et al.*, 2019), as well as from MODIS (Moderate Resolution Imaging Spectroradiometer) images from Terra and Aqua satellites (Novillo *et al.*, 2019; Zhang *et al.*, 2003), and even high-resolution studies from the Landsat and Sentinel image series satellites (Fisher *et al.*, 2006; Vrieling *et al.*, 2018), have been particularly used. Phenological parameters are usually extracted using different vegetation activity indicators derived from radiometric information. Among the most used indicators are the NDVI (Normalized Difference Vegetation Index), EVI (Enhanced Vegetation Index), or LAI (Leaf Area Index), among others (Karkauskaite *et al.*, 2017; Verger *et al.*, 2016; Zhang *et al.*, 2003). From these indices, phenological variables corresponding to the start of the season, the end, or the duration of the same can be extracted, provided the observations have been taken with an adequate temporal frequency. These variables are also called phenometrics. There are different methodologies and algorithms for phenological analysis (Jönsson and Eklundh, 2002; Sakamoto *et al.*, 2005; White *et al.*, 2014), but all of them obtain the phenometric variables from time series of vegetation indices through three stages: i) improving the quality of the input indices, ii) fitting functions to the vegetation cycles, and iii) identifying the start and end dates of the growing season by establishing thresholds or inflection points (Liu *et al.*, 2016), from which to derive other phenological variables.

In Spain, studies have analyzed vegetation dynamics in recent decades, mainly through long series of observations in some specific locations (García-Mozo *et al.*, 2010; Gordo and Sanz, 2009; Peñuelas *et al.*, 2002). The results of these studies suggest phenological changes due to the current warming process (Caparros-Santiago and Rodríguez-Galiano 2020; Gordo and Sanz, 2009). Although there have been some approaches to characterize Spain's phenology from satellite images (Alcaraz Segura, 2006; Amorós-López, *et al.*, 2013; Caparros-Santiago and Rodríguez-Galiano 2020; Gutiérrez-Hernández, 2020; Martínez and Gilabert, 2009; Novillo *et al.*, 2019), the studies have covered short periods. For this reason, this study addresses the study of plant phenology in Spain over the last four decades using satellite image series at a medium spatial resolution (1.1 km^2), which is considered sufficient to determine possible patterns of change based on a good number of vegetation phenology parameters.

The objectives are to spatially characterize the phenology of vegetation in Spain in the long term and determine, from a set of phenological variables, both its average conditions and variations over time and space, as well as the changes recorded since the beginning of the 1980s in mainland Spain including the Balearic Islands.

2. Data and methods

2.1. Study Area

The study area encompasses mainland Spain, including the Balearic Islands. From an ecological perspective, Spain can be divided into two macro-biogeographic regions: Mediterranean and Eurosiberian. The Eurosiberian zone covers the northern and northwestern territories, as well as mountainous areas, while the remainder of the country falls within the Mediterranean region. Spain is also one of Europe's most diverse territories, not only in terms of its natural environment but also in its land use, which is highly varied (Fig. 1). In the Mediterranean region, vegetation comprises many functional plant types whose phenological responses vary according to environmental signals, with temperature being the key factor for most species (Peñuelas *et al.*, 2002). However, it is the summer drought in the peninsula that controls the vegetative activity in the Mediterranean area, with the growth phase occurring during the cooler, wetter part of the year (Matesanz *et al.*, 2009; Prieto *et al.*, 2008); unlike the Eurosiberian region, which exhibits growth during warmer temperatures.

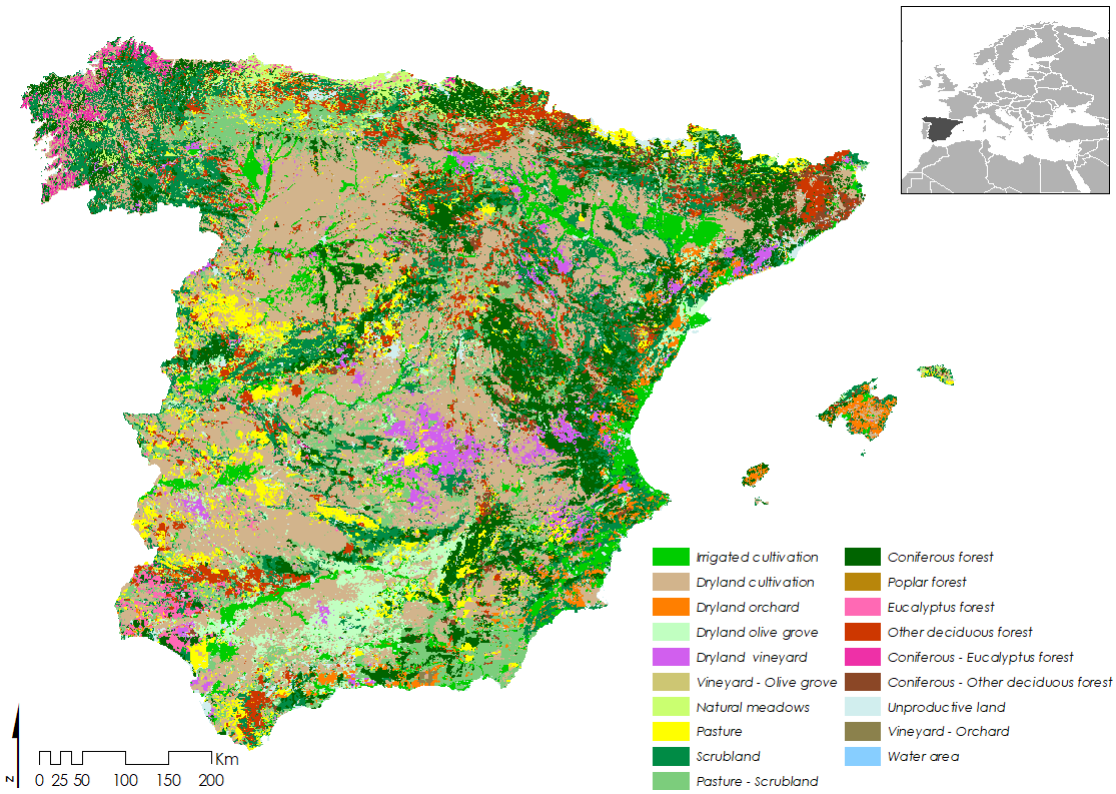

Figure 1. Map of crops and uses, 1980. Source: MAPA.

2.2. Generation of a 40-Year NDVI Time Series

The foundational data for this study were two databases of the Normalized Difference Vegetation Index (NDVI). The first database was generated from NOAA-AVHRR satellite images from 1981 to 2015, developed through georeferencing, calibration, and radiometric correction of over 10,000 satellite images. This database offers a spatial resolution of 1.1 km² and a semi-monthly temporal frequency, with two images each month made from the composites of the daily images available. This database does not exhibit information gaps. Complete information on this database can be consulted in Vicente-Serrano *et al.* (2020). The second database comes from MODIS (Moderate Resolution Imaging Spectroradiometer) satellites for the period 2001-2021. NDVI data are from the MOD13A2 product and are available at a spatial resolution of 1 km and a temporal frequency of 16 days. Complete information on the database can be found at https://lpdaac.usgs.gov/products/mod13a2v006/. To analyze long-term phenology (between 1981 and

2021), it was necessary to combine both sources of information. This involved transforming the spatial resolution of the MODIS images (1 km) to match the 1.1 km of the NOAA-AVHRR images, considering the same envelope and spatial extension through bilinear convolution. Subsequently, it was necessary to transform the temporal frequency of the MODIS images from their temporal location every 16 days to the fixed frequency of the NOAA-AVHRR images (one image corresponding to days 1-15 and another from 16 to the end of the month). A linear interpolation process of the image values was applied on a daily basis, and the average NDVI within the same temporal intervals as the database from the NOAA-AVHRR images. Due to the significant difference, both in the total magnitude of NDVI and in its annual range of variation, between both databases (Fig. S1), a fusion of the data was performed to adapt the NDVI data from the NOAA-AVHRR images to those of the MODIS images.

To carry out the fusion of both databases, the NDVI series were transformed into standardized values, using the common period 2001-2021. Different probability distributions (exponential, Gamma, log-normal, Weibull, Pearson-III, normal, general Pareto, general normal, general extreme values, and general logistic) were tested for the adjustment of each of the semi-monthly series for each of the pixels in the database. The equations for these distributions can be consulted in Vicente-Serrano *et al.* (2012). The selection of the most suitable distribution for each pixel and semi-monthly series was made using the highest value of the Shapiro-Wilks test with the aim of obtaining standardized values, which perfectly follow a standard normal distribution according to Stagge *et al.* (2015).

Finally, the anomaly series from the NOAA-AVHRR images were transformed into NDVI values based on the parameters obtained from the MODIS series of the common period. This procedure allowed obtaining AVHRR series perfectly comparable in terms of magnitude and variability range of the MODIS NDVI series, with a high degree of adjustment during the common period (Fig. S2). In the common period, the MODIS image series from the year 2001 were preserved, so the NOAA-AVHRR images contained in the final database correspond to the period 1981-2001. Figure S3 shows, using the D index (Willmott, 1981), the analysis of the goodness of the reconstruction in a spatial and summarized manner for different periods of the year and land uses. The maps of the index in different weeks show a predominance of values above 0.6 throughout Spain, meaning that the reconstructions are generally acceptable, and quite good in broad regions showing values close to 1. In fact, the reconstruction presents less uncertainty on the scale of specific weeks, and particularly during the summer, when the reconstructed NDVI values from the AVHRR images show a high degree of adjustment with the NDVI data from MODIS. The differences between semi-monthly periods are scarce, although the reconstruction is better for the summer months, and no significant bias is observed in the goodness of the reconstructions among different land uses. Although there are some uncertainties in the reconstruction at the local level, it can be considered that the procedure used provides very acceptable results and allows the use of the series for the estimation of phenological parameters over the last four decades.

2.3. Calculation of Phenological Variables

For the analysis of vegetation phenology, 960 semi-monthly periods from 1983 to 2021 were worked with. Applying time series analysis algorithms of vegetation indices implemented in TIMESAT (https://web.nateko.lu.se/timesat/timesat.asp), a series of 13 plant phenology parameters were extracted: date of the start of the season, date of the end of the season, mid-season date, duration of the season, the maximum index value in the season, the index value at the start date, the index value at the end date, base value (average of the start and end of season values), amplitude (difference between the maximum and base value), left derivative, right derivative, large integral (area under the curve for the entire season), and small integral (area under the curve for the entire season relative to the base value) (Eklundh and Jönsson, 2017; Jönsson and Eklundh, 2002).

For the fitting of functions to the NDVI series, a Savitzky-Golay filter (Kim *et al.*, 2014) with a moving window size of 2 was used, which is conservative in relation to the maintenance of the original

NDVI data. This filter was chosen because it is more accurate and advantageous in periodic time series and particularly in processed NDVI series, as these are relatively unaffected by atypical observations (Eklundh and Jönsson, 2017). Likewise, by using this filter, more complex behaviors can be distinguished as it closely follows seasonal changes, by iteratively adjusting the window that captures the increase and decrease of the data (Eklundh and Jönsson, 2015). Additionally, this procedure is effective in characterizing certain soil covers, such as semi-arid grasslands that change their activity in short periods of time (Jönsson and Eklundh, 2004).

A key aspect in determining phenological cycles is establishing the start and end of the vegetative season. For this, a test was conducted based on different soil covers considering the amplitude of the vegetative season, defined between the base level and the maximum value of the data distribution for each season. The start occurs when a specified fraction from the left of the adjusted curve relative to the base level is reached, set at 0.3 units since this value shows a good fit for different soil covers at the national level. Conversely, the end of the season was defined at a value of 0.2, which showed more consistent results in different soil covers such as deciduous forests, grasslands, rainfed crops, etc. The preliminary analysis of the data allowed verifying that, given the characteristics of some of the covers and certain phenological cycles, the model obtained incoherent results in some areas, with very variable vegetative activity seasons, like certain irrigated crop areas. In order to eliminate the data where the confidence in the phenology estimation was very low, the areas where the interannual deviation corresponding to the start date data was greater than 75 days (5.3% of the study area) were removed, as the uncertainty of the phenological estimates in these areas was very high. Also, the first and last year of the time series of all phenological variables were removed to avoid artifacts in the estimation of incomplete phenological periods, so the temporal analysis was finally limited to the period 1983-2020.

2.4. Analysis of Vegetation Phenology

The analysis of the different phenological variables was based on the spatial characterization of the phenological variables through averages and coefficient of variation. To evaluate changes in the different variables, two non-parametric statistics were used: the Theil-Sen regression to estimate the trend, a consistent method for asymmetric distributions and with high tolerance to error deviations (Fernandes and Leblanc, 2005; Peng *et al.*, 2008), and the Mann-Kendall test (Mann, 1945; Kendall, 1948), which allows determining the statistical significance of the observed changes in the trends of the variables. A significance threshold $\alpha = 0.05$ was used. The results were obtained for each of the 1.1 km pixels, but a grouping of the results for the main soil covers of Spain was also carried out. For this, the crop and land use map between 1980 and 1990 at a scale of 1:50,000 generated by the Ministry of Agriculture, Fisheries and Food (MAPA, https://www.mapa.gob.es/es/cartografia-y-sig/publicaciones/agricultura/mac_1980_1990.aspx) was used.

3. Results

The average start of the vegetative activity season exhibits clear spatial differences between the Eurosiberian region, some mountain areas of inland Spain, and certain irrigated zones, which begin their season at the end of the first quarter of the year, and the rest of Spain's vegetation, the Mediterranean, which starts its season between September and November (Fig. 2). During the study period, a strong interannual variation in the season's start is observed in the Duero basin and the Southern Plateau, corresponding to rainfed areas, and the irrigated zones of the Guadalquivir and Ebro, as well as most of Galicia. The magnitude of change shows negative values across most of Spain, suggesting an advancement in the start of vegetative periods, between 1 and 2 days per year and exceeding 2 days in some areas of the northern and southern plateaus and in the Guadalquivir valley. Conversely, a delay in the start of vegetative activity of between 1 and 2 days per year is observed in Galicia. The changes in these areas are statistically significant.

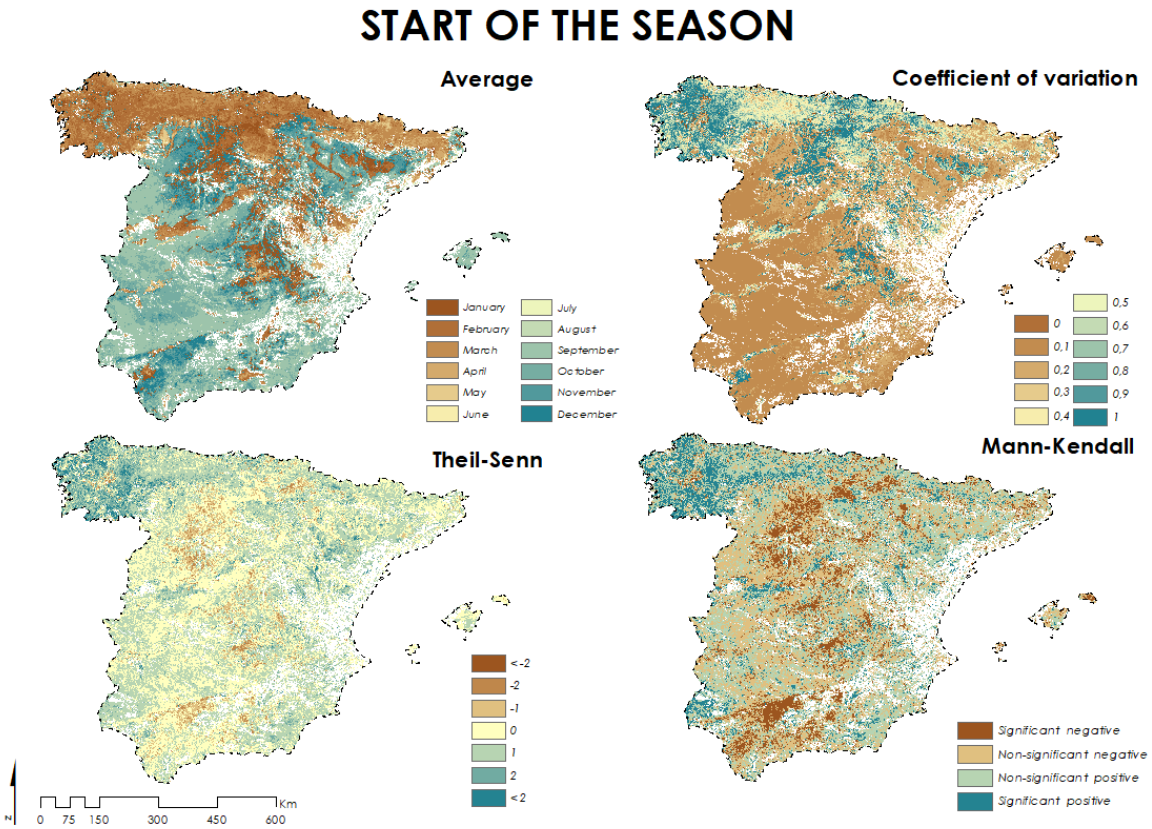

Figure 2. Maps of the statistics for the start of the season.

The analysis by different land covers shows high variability in the average start dates of the season for some cover types (Fig. 3 a)), suggesting broad subregional differences. Irrigated lands, vineyards, rainfed areas, scrublands, conifers, eucalyptus, and deciduous forests, among others, have a very asymmetric distribution of the average. The lowest variability in the average start date of vegetative activity is presented by natural meadows, grasslands, some rainfed crops, and mixed forests of eucalyptus with conifers. The highest interannual variability in the start of vegetative activity (Fig. 3 b)) is recorded in mixed forests of eucalyptus with conifers and in natural meadows, and the lowest variability is recorded in rainfed crops. In general, the trend for all land covers has been towards an advancement in the start date of the vegetative season, especially in areas of poplars and willows and irrigated surfaces.

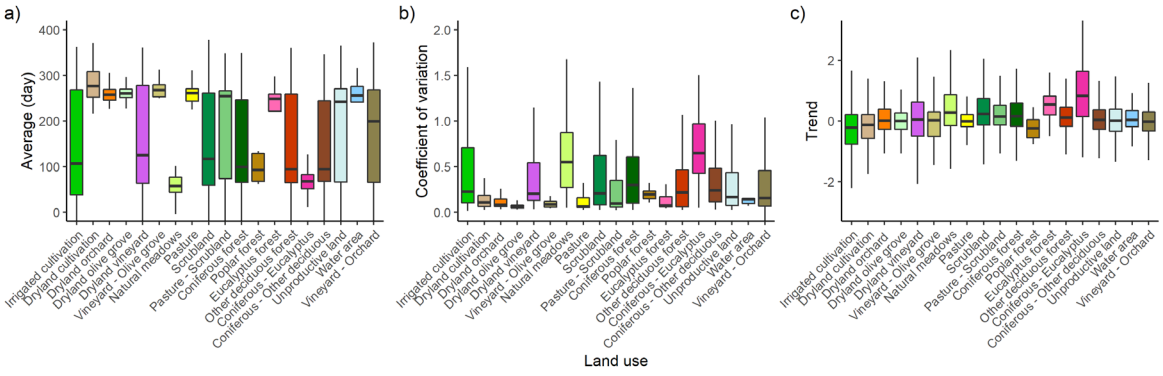

Figure 3. Season start statistics throughout the series according to different types of land cover.

The percentage of surface area showing statistically significant changes in each of the land covers indicates that nearly 50% of Spain's eucalyptus surface area has delayed the start of the season. The same occurs in 40% of the extension of mixed forests of eucalyptus with conifers and in 20% of natural meadows (Fig. 4). On the other hand, it is notable that around 20% of the areas of rainfed and irrigated crops and natural riverbanks show a significant advancement in the start dates of vegetative activity.

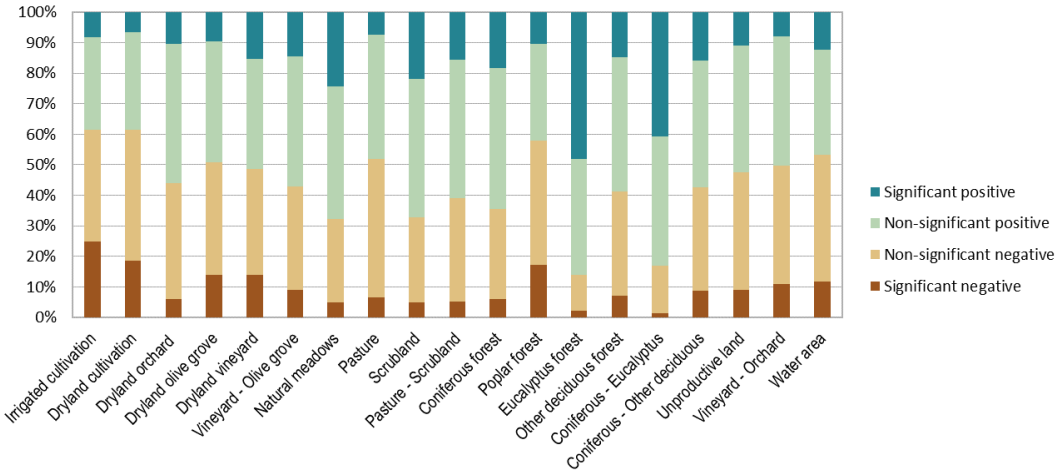

Figure 4. Changes in season start by land use.

The end of the season also presents notable spatial differences (Fig. 5). In general, the interannual variability of the end date of the season is low and very homogeneously spatially across the country. However, the magnitude of change indicates negative variations in the floodplains of the large rivers, where the end of the season advances between 1 and 2 days per year; with even greater advancements in areas located along the riverbanks. Conversely, in areas of Galicia and Extremadura, a delay of between 1 and 2 days per year is observed during the study period.

The analysis performed based on the different land covers shows a great difference in the average end date of the season (Fig. 6 a), suggesting subregional differences. The variability of the end of the vegetative period is low in all covers, being the most variable the irrigated zones and conifers with eucalyptus (Fig. 6 b). The trend is practically null in all covers. However, mixed forests of conifers with eucalyptus present a clear tendency to delay the same (Fig. 6 c).

It is important to highlight a delay in the end of the season in 35% of the surface of mixed forests of eucalyptus with conifers and 20% of the surface of eucalyptus (Fig. 7). Around 10% of all surfaces have delayed their senescence. Whereas in the areas of irrigated land, rainfed farming, and natural riverbanks, this date has been advanced in 30% of the surface.

The average date of mid-season follows a very marked spatial pattern: the northern area has its mid-season in summer, while in the rest of Spain, it occurs during winter and early spring (Fig. 8). The analysis of the magnitude of change shows an advancement of the mid-season date in irrigated areas around the riverbanks. This advancement is 2 days per year since the beginning of the 1980s, while in the rainfed areas of the Duero and Guadalquivir valleys, the advancement is usually about 1 day. Conversely, in Galicia and the Ebro valley, a delay of around 1 day per year is observed.

The analysis by different covers shows high variability in the mid-season date in all of them, with greater subregional differences in vineyard areas, scrublands, conifers, and deciduous forests (Fig. S4). Most covers have their mid-season between January and March (month 1 and month 3), except natural meadows, conifers, deciduous forests, and mixed forests of conifers with eucalyptus and other deciduous trees, which tend to register the mid-season date around July. The trend in all covers is the advancement of this date. Similarly, a higher percentage of surface area advancing the mid-season date has been identified in most land uses (Fig. S5).

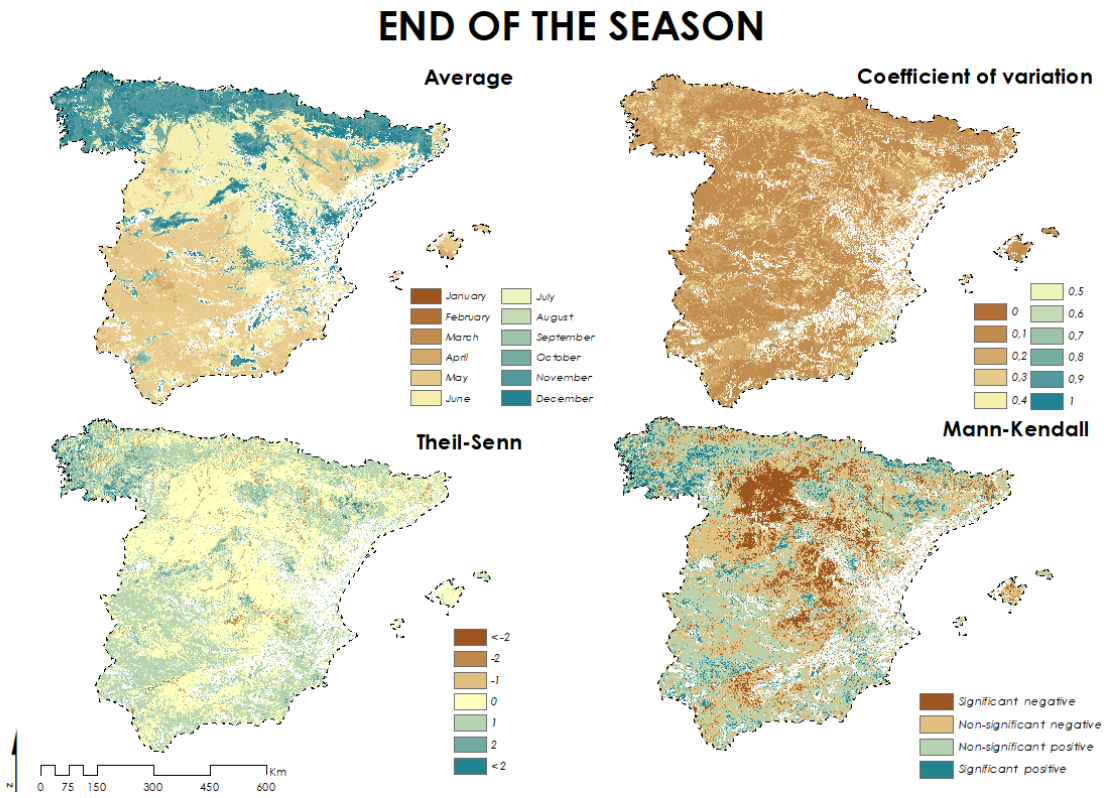

Figure 5. Maps of the statistics for the end of the season.

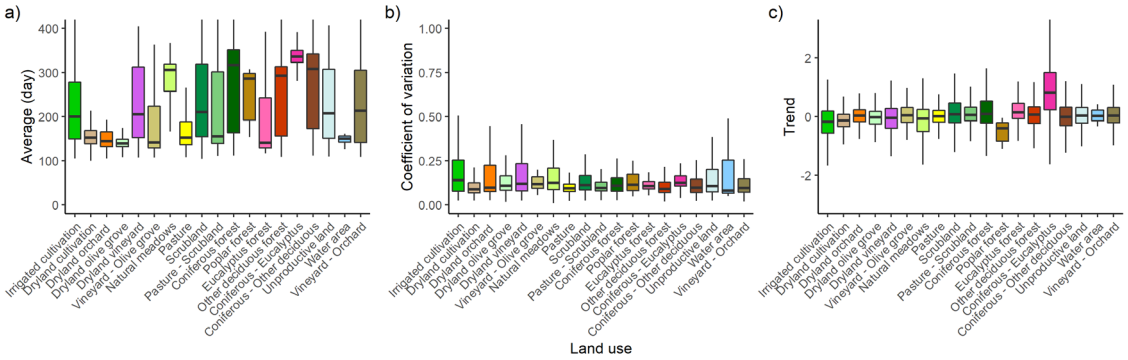

Figure 6. End-of-season statistics throughout the series according to different types of land cover.

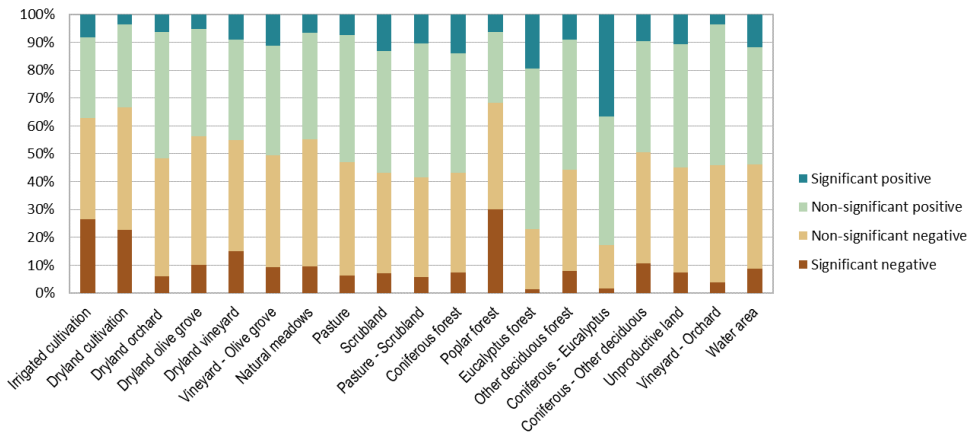

Figure 7. Changes in the end of season by land use.

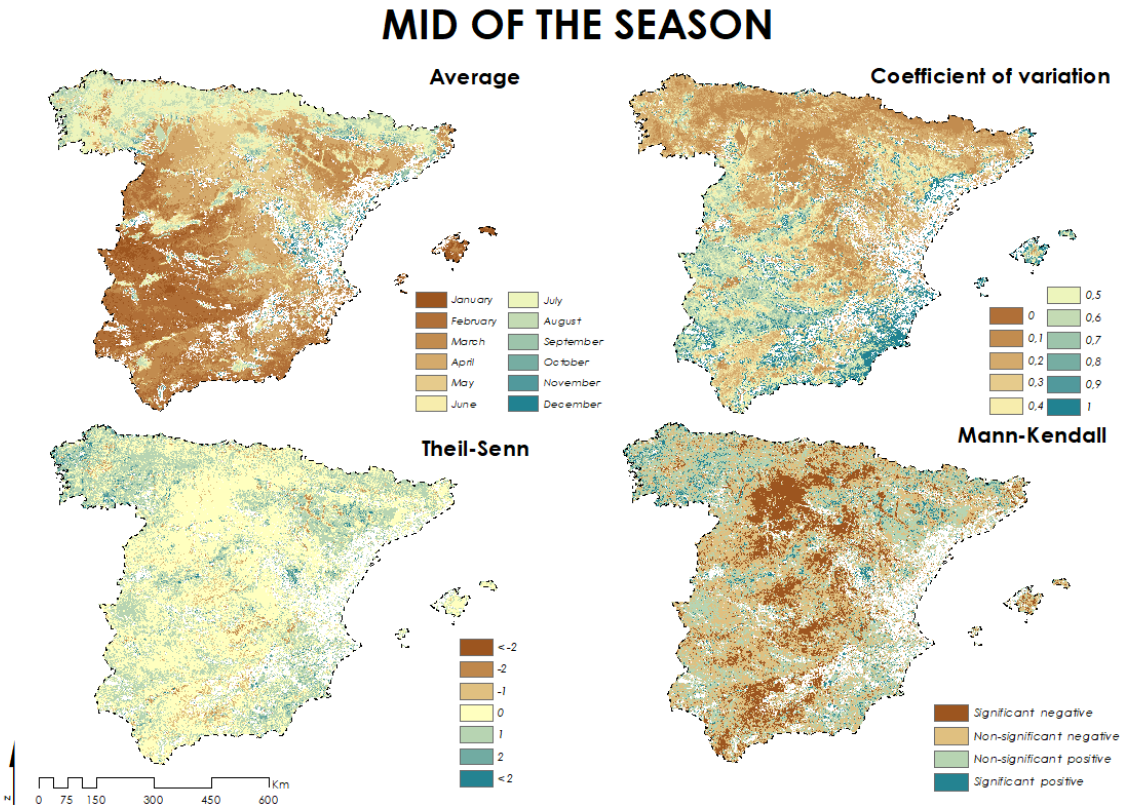

Figure 8. Maps of the statistics for the mid-season date.

The average duration of the vegetative activity season in Spain is between 7 and 9 months, except in the interior areas of the large basins, where the season lasts about 6 months (Fig. 9). The interannual variability in the duration of the season series marks a southeast-northwest line starting in the region of Murcia and ending in Galicia, dividing the study area into two parts, with the area north of the line characterized by greater variation over time. The magnitude of change shows, in general, an increase of 1 day in the duration of the season per year, except in the north and in some of the interior Mediterranean mountain ranges where the duration has decreased by 1 day or more, especially in Galicia. The changes in these areas tend to be statistically significant, especially in areas of the Guadalquivir valley.

In the analysis conducted for the different covers, it is noteworthy that the average duration of the vegetative season is very homogeneous, between 6 and 8 months (Fig. S6), and presents few subregional differences. Notable interannual variability is detected in all covers, being the most variable annually the irrigated crops and poplar and willow groves. Most covers show a dominance of negative values in the magnitude of change of the vegetative period, especially in natural meadows and poplars and willows, while the duration of the vegetative season increases in rainfed farming, olive groves, vineyards, and grasslands.

Between 5% and 10% of the surface area of all soil types has experienced a significant decrease in the duration of the vegetative season (Fig. S7). Notably, natural riverbank areas and eucalyptus forests have done so in more than 15% of their surface area. On the other hand, irrigated areas are those with the most surface area (10%) showing an increase in the activity period, along with rainfed surfaces and grasslands.

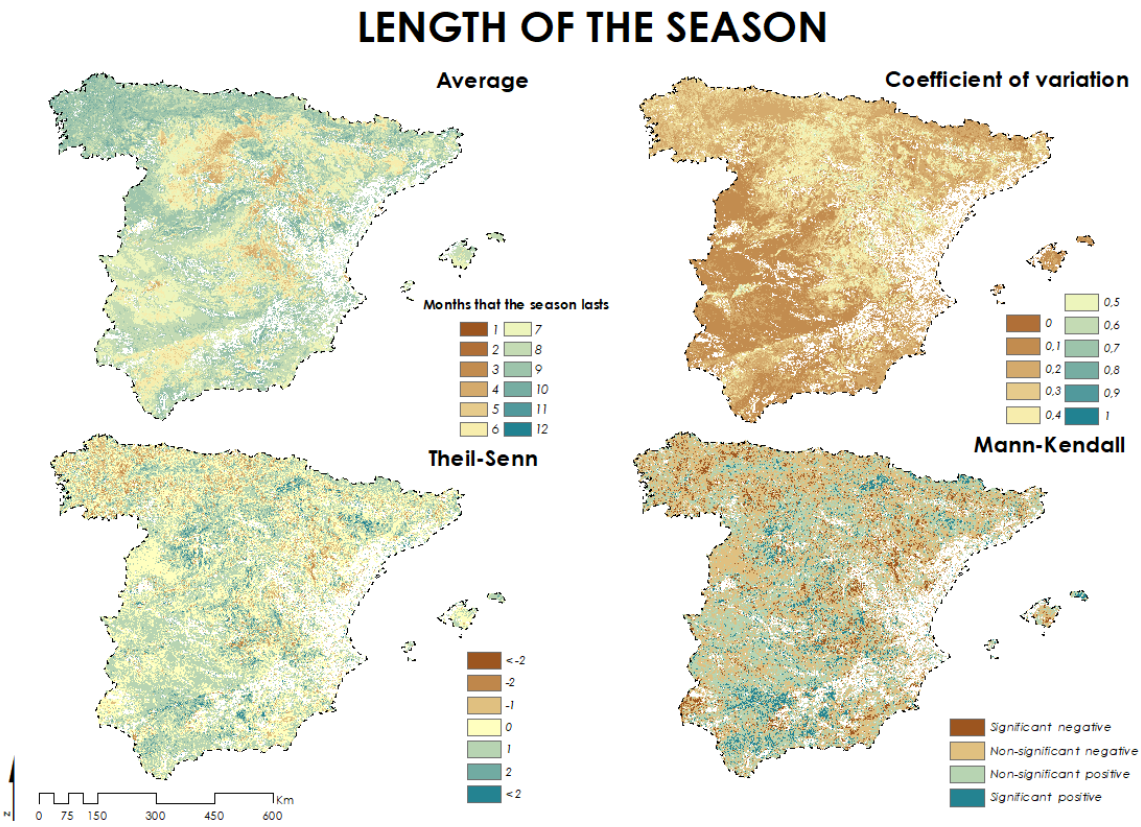

Figure 9. Maps of the statistics for the duration of the vegetative season.

The average base value of NDVI presents very notable spatial differences (Fig. 10). On one hand, Galicia, the Atlantic coast, and the Pyrenees show very high base values, while the rest of Spain has a much lower value. The Cantabrian Mountains, Pyrenees, and Sierra Nevada stand out in their base value with a base value of 0. Its variability is very high in the northern area, the Iberian System, and some irrigated areas. It presents positive variations in most of Spain, increasing more than one-hundredth per year, except in the Southern Plateau and the Duero Basin where the value remains the same or decreases slightly. The changes in almost all of Spain are positive and statistically significant, so it can be stated that the NDVI values at the start and end of the season are generally increasing.

The highest average base values are observed in eucalyptus with conifers and natural meadows, while the lowest occur in rainfed crops (Fig. S8). The interannual variation in the base value tends to be low, and the general trend of all covers is towards an increase in this metric.

There is a statistically significant increase in base value in 50% or more of the surface area of all covers (Fig. S9). Irrigated areas, vineyards, and eucalyptus stand out from the rest of the covers where the change in their surface is smaller, and especially coniferous forests and other deciduous forests, in which 80% of their surface area has seen this value increase.

The average maximum NDVI value presents clear spatial differences between the northern and western part of the country, where values are higher (0.7-0.8), and the eastern zone where they are much lower (0.2-0.5), highlighting the Ebro basin, as well as the regions of Almería, Murcia, and La Mancha (Fig. 11). The interannual variability of the season's maximum is low, with greater variation observed in the basins of the Ebro, Duero, Guadalquivir, and in the Southern Plateau. The magnitude of change of the maximum value shows an increase of more than one-hundredth of NDVI each year, except in the Guadalquivir valley and small areas in the center of the country where the value decreases more than one-hundredth. The changes in almost all of Spain are statistically significant.

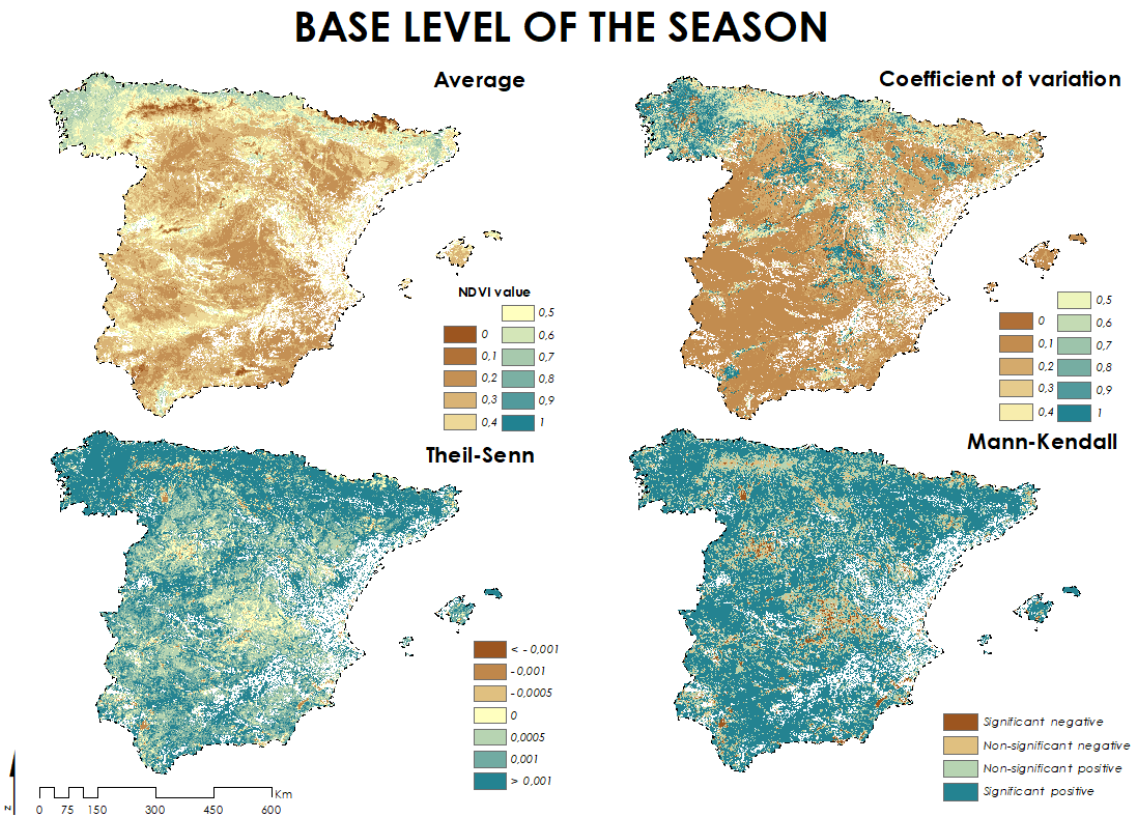

Figure 10. Maps of the statistics for the base value of the season.

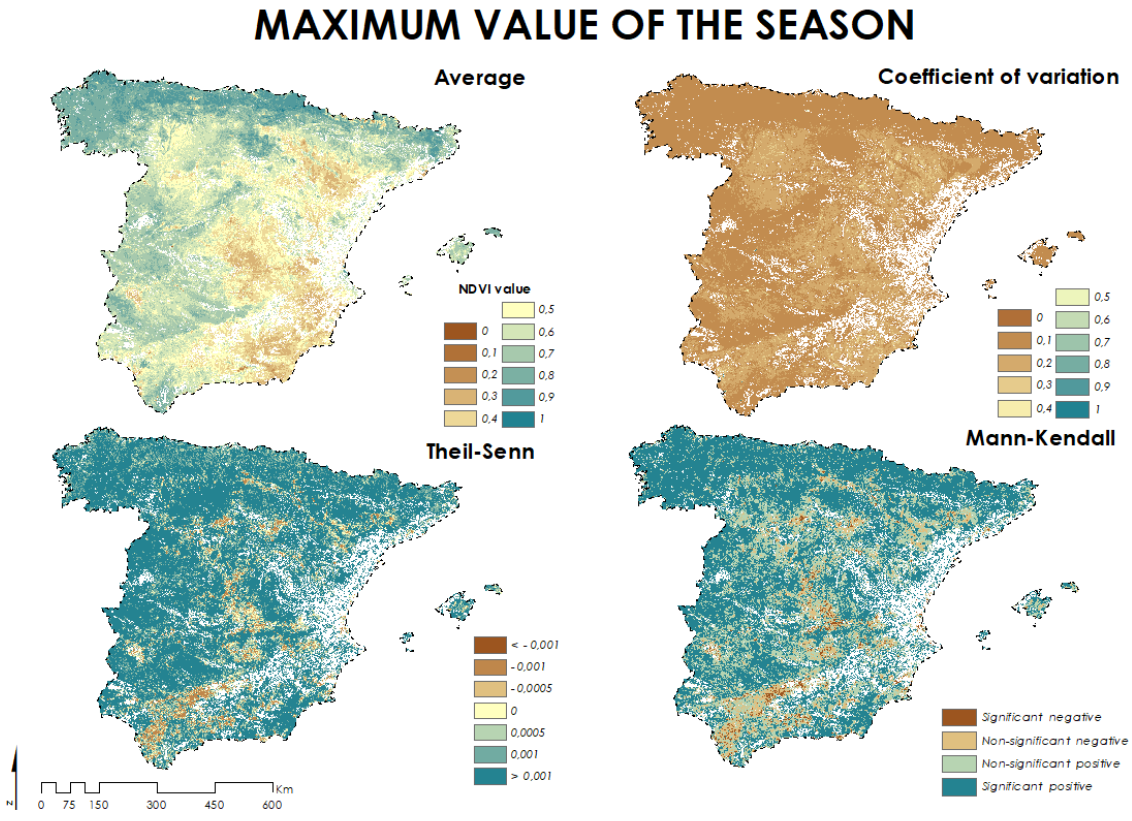

Figure 11. Maps of the statistics for the maximum value of the season.

The highest average maximum NDVI values in the different land covers are recorded in natural meadows, deciduous forests, and eucalyptus with conifers, and the lowest in rainfed crops (Fig. S10). The interannual variations are low, with rainfed farming being the most variable cover and natural meadows and conifers with eucalyptus being the least variable. The trend in all soil covers is towards an increase in the maximum NDVI value. The maximum NDVI value has increased in at least 45% of the surface area of all categories (Fig. S11), with conifers and natural meadows being the categories where the surface area affected by significant changes is higher (80%).

The average amplitude of NDVI values shows homogeneity across Spain, with values between 0.2 and 0.3 in most of Spain (Fig. 12), except in the Cantabrian and Pyrenean ranges, with amplitudes higher than 0.6, and areas in the west of the country, with amplitudes around 0.5. The interannual variability of this variable is low in areas where the amplitude is higher, while it is higher in the east of the country and in the northern area of Galicia. The magnitude of change shows a decrease of one-hundredth in the amplitude each year in the north, in the Central System, and in part of the Guadalquivir depression, while in the rest of Spain, it increases by one-hundredth. In wide areas of the interior of Spain, there is a statistically significant increase in the annual amplitude of NDVI values throughout the study period, as well as significant decreases of NDVI in the northern part of the country.

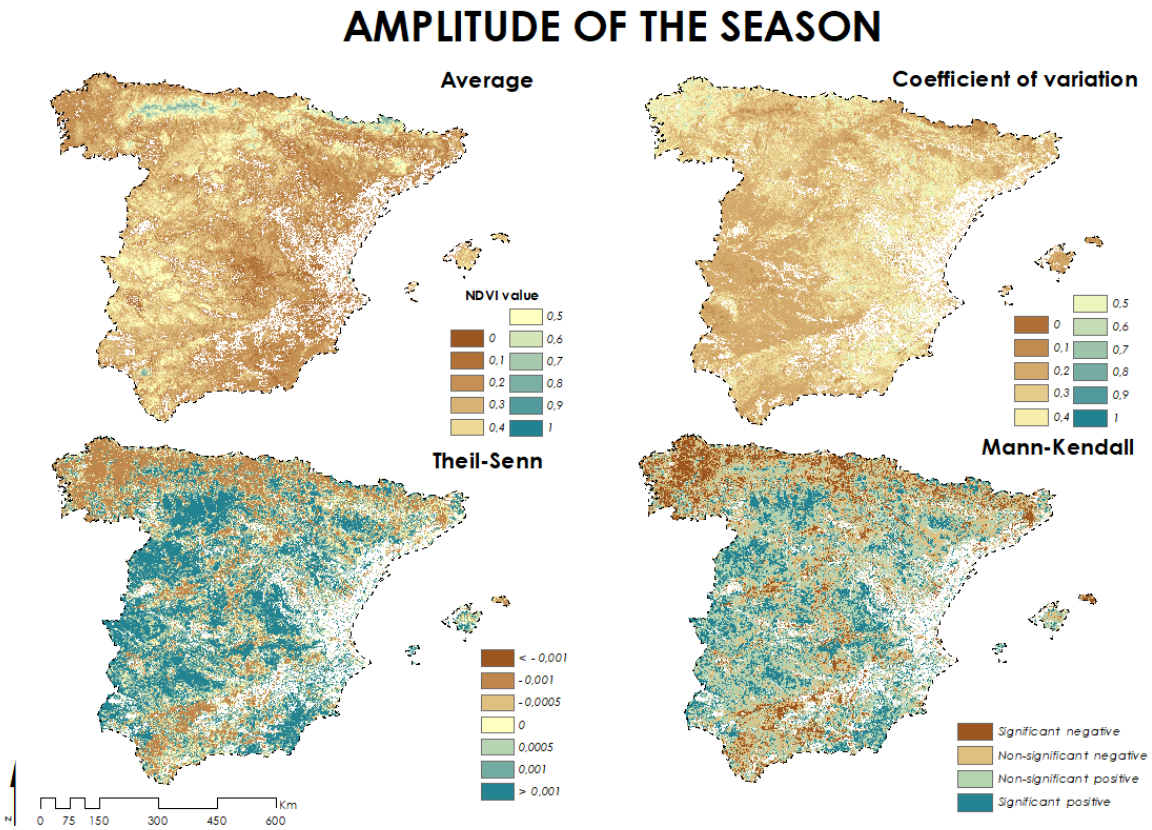

Figure 12. Maps of the statistics for the amplitude of the season.

The average amplitude among the different covers is very similar (Fig. S12). Similarly, the interannual variability of the NDVI amplitude is similar in the different soil classes, although it tends to be higher in mixed areas of conifers and eucalyptus, in dry vineyards, and in grasslands. The trends of this variable are similar in all covers, positive, except for natural meadows and forests of eucalyptus with conifers showing dominant negative trends. All covers have experienced an increase in amplitude in at least 5% of their surface area (Fig. S13), while also suffering a decrease in almost 10% of their surface area. Vineyards with fruit trees stand out where 50% of their surface area has experienced

increases in amplitude and olive groves and dry fruit trees have done so in 30% of the surface area. On the contrary, natural meadows, mixed forests of conifers with eucalyptus, and poplars and willows are the covers that have seen a reduction in amplitude on a larger surface area, of 30%.

The evolution of other secondary phenological variables also shows some relevant results. For example, the rate of decline at the end of the season (right derivative) (Fig. S14) and the rate of growth at the start of the same (left derivative) (Fig. S15), show very notable spatial differences, with higher average values in the Pyrenees and Cantabrian Mountains, as well as in the most western regions of Spain. Conversely, the average values are lower in the eastern zone. The data present high interannual variability for both derivatives, observing very high variation coefficients of the right derivative in the northern area of Spain and of the left derivative almost in the entirety of the country. The magnitude of change of the two derivatives shows a decrease in the rate of one-hundredth in Galicia and interior Mediterranean mountain areas and an increase of one-hundredth in the west of Spain. All changes tend to be statistically significant. The analysis by different soil covers (Fig. S16 and S17) shows very similar averages, being the grasslands the ones presenting the highest average rates, and natural meadows and conifers with eucalyptus the ones that have varied the most. These two covers are the ones presenting a negative trend, both their start and end rate of the season have decreased, as have also done the areas of riparian forests, while in the rest the rates have remained or increased. The percentage of surface area showing statistically significant changes in each of the covers is similar in both derivatives (Fig. S18 and S19), although there is more surface area affected by an increase in the start rate.

The analyses of the large integral (Fig. S20) present the same spatial differences as the maximum NDVI value, distinguishing the northern and western areas, which show the highest values, and on the other hand the river basins and the east of the country, which present the lowest values. There is a dominance towards the increase of the area of the integral, being the changes predominantly significant. The large integral presents a similar variation and a positive trend in all soil covers (Fig. S21). The percentage of surface area showing statistically significant changes for each of the soil covers shows an increase in the integral in 20% of the surface area of all covers, finding the maximum surface area affected in dryland and grassland areas in 40% of their surface area (Fig. S22). On the other hand, the small integral (Fig. S23) shows higher values in the Cantabrian Mountains and the Pyrenees, as well as in the western part of the country. The variability is high throughout the country, except in the southwest. The magnitude of change and its significance show a decrease in the north of the country and an increase of the variable in the rest. All surfaces present the same pattern in the small integral (Fig. S24) and without a very contrasting behavior between soil covers on the surface characterized by significant changes (Fig. S25).

The initial average value of the season (Fig. S26) is practically the same as the average base value and very similar to the average end value of the season (Fig. S27). Although it is true that the coefficient of variation is very low in initial and final values compared to the base value, the magnitude of change and the significance is the same or greater, that is, in all three there is a notable increase in NDVI throughout the country except in part of the Guadalquivir basin and the Southern Plateau. The analyses by different soil covers in the initial and final values (Fig. S28 and S29) are practically the same among them and compared to the analysis of the base value. Similarly, the figures for percentages of soil affected by significant changes (Fig. S30 and S31) mostly present more than 50% of the surface area of all covers with a significant increase in the variables and practically no effect by the decrease of this.

Generally speaking, the percentage of surface area with statistically significant changes in each of the variables does not demonstrate a clear dominance towards temporal changes in the start and end of the vegetative period (Fig. 13). However, there has been a dominant significant increase in NDVI values (base, maximum, start, and end of the season) that has affected between 60% and 70% of Spain's surface area. Likewise, the mid-season date advances almost in 20% of Spain and the NDVI amplitude

throughout the season has had similar significant positive and negative changes, although the amplitude increases in 10% more surface area than it decreases.

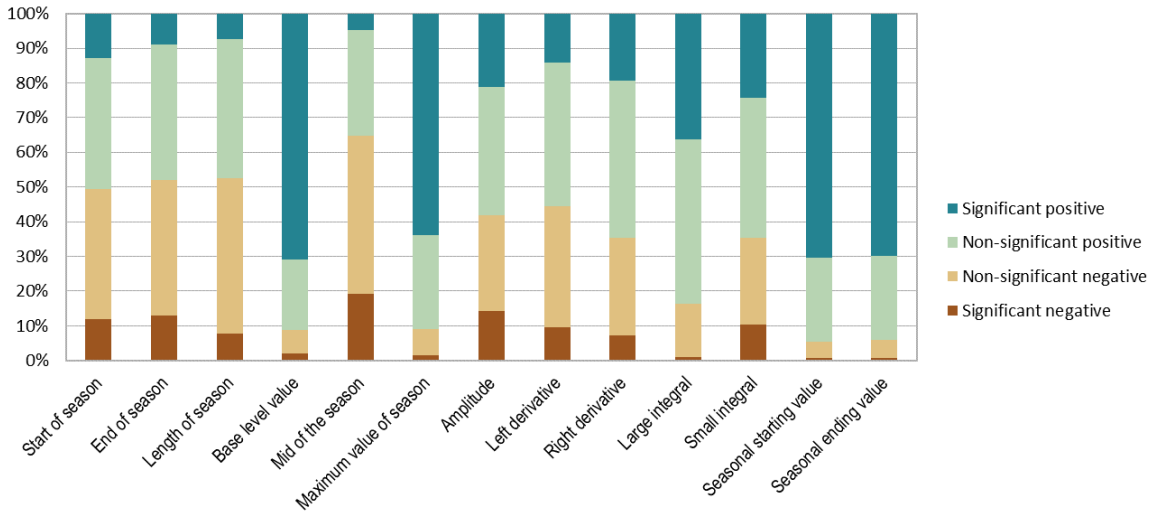

Figure 13. Percentages of changes in the total surface area of Spain for the 13 phenological variables extracted from TIMESAT.

4. Discussion and conclusion

This study analyzed plant phenology in Spain from the early 1980s to the early 2020s, using low and medium-resolution satellite imagery based on a database developed for this purpose that merges NDVI values obtained from NOAA-AVHRR and MODIS images. The interest in such studies is significant from an environmental perspective, as various continental and global studies since the 1980s suggest phenological changes in response to climate change (Bertín, 2008).

Previous studies on phenology in Spain have focused on specific locations within the country, particularly in the Mediterranean region (García-Mozo *et al.*, 2010; Gordo and Sanz, 2009; Peñuelas *et al.*, 2002). Although there are recent studies covering the entire peninsula (Alcaraz-Segura *et al.*, 2009; Caparros-Santiago and Rodríguez-Galiano, 2020; Novillo *et al.*, 2019), they have been conducted over shorter time periods. For this reason, a robust database was developed to allow for phenological analysis in Spain based on biweekly NDVI data from 1981 to 2021, enabling a study with a broad temporal perspective. This study does not delve into detail but analyzes general patterns of different phenological variables at the national level that may allow for future detailed analysis of the identified changes (e.g., using higher spatial resolution sensors) and to determine the role of observed climate changes on plant phenology, as suggested by various previous studies (Lunetta *et al.*, 2006; Zhang *et al.*, 2017; Fu *et al.*, 2014; Jeong *et al.*, 2017; Piao *et al.*, 2019).

The methodology of this study was based on the TIMESAT tool (Eklundh and Jönsson, 2017), which allowed for the processing of approximately one million pixels to study phenology in satellite image series with extensive temporal coverage. Phenology was characterized from NDVI series as objectively as possible. This is not straightforward, as thresholds for defining the start and end of the vegetative season can vary. For example, changes in coniferous forests are slow, but in semi-arid grasslands, they are very rapid, creating problems in capturing seasonal changes in various types of cover. This means there are no universal thresholds for defining the start and end of the season (Eklundh and Jönsson, 2015). Thus, for this work we had to establish thresholds that allowed the objective evaluation of the phenological variables of interest. One limitation observed in the applied methodology was the difficulty in analyzing spaces with high interannual variability; variability that could be due to

land use changes caused by urban expansion and tourist infrastructures, especially on the Valencian coast (Marraccini *et al.*, 2015; Palazón *et al.*, 2016), an increase in irrigated area, changes in sowing decisions (Oteros *et al.*, 2015; Stellmes *et al.*, 2013), the succession of forest fires (Díaz-Delgado *et al.*, 2002), or the difficult detection of changes in evergreen coniferous forests (Eklundh & Jönsson, 2015).

The main results of the phenological analysis of Spain highlight that the start of the season has advanced in wide areas by between 1 and 2 days per year. These are considerable figures that suggest significant phenological changes are occurring in Spain. The most affected covers by this early start are natural riverbanks and rainfed and irrigated crops. These results are consistent with those observed in previous studies like those of Caparros-Santiago and Rodríguez-Galiano (2020) and Oteros *et al.* (2015), which also detected this dominant advancement through both remote sensing and field data. These studies suggest that such advancement could be related to the increase in air temperature (Oteros *et al.*, 2015). Additionally, this trend coincides with various studies conducted in Europe (Ahas *et al.*, 2002; Stöckli and Vidal, 2004), North America (Reed, 2006), Asia (Piao *et al.*, 2006), and across the Northern Hemisphere (De Beurs and Henebry, 2005; Eastman, *et al.*, 2013; Jeong, *et al.*, 2011; Zhou *et al.*, 2001), all emphasizing an early advancement since 1960 in the start of the season, both in satellite observations and ground observations, but whose magnitude differs according to the study region, scale, period, and species (Piao *et al.*, 2019).

Notable subregional differences were found in this work. For example, in areas of eucalyptus, conifers, natural meadows, and deciduous forests, there is a certain delay in the start dates of vegetative activity, results that also align with the regional outcomes of Caparros-Santiago and Rodríguez-Galiano (2020) and Jato *et al.* (2002), which could be due to changes in air temperature (Lieth, 1974; Cleland *et al.*, 2012).

The results reveal a certain concordance between changes in the start and end of the season. In places and covers where the start of the season advances between 1 and 2 days per year, so does the end of it in a similar interval, except for river forest areas where the advancement is more than 2 days per year. Meanwhile, delays between 1 and 2 days are observed in areas of Galicia and Extremadura, especially in surfaces of eucalyptus and broadleaf and mixed forests of both with conifers. In general, trends towards a certain delay and advancement in the end of the vegetative season have been evidenced, although in a weaker magnitude than the change in the start of the season. In this sense, and although there are fewer local, regional, and global studies focused on this, it is important to note that most of them agree in showing a dominant delay in wide regions of temperate climates (Miao, *et al.*, 2017; Piao *et al.*, 2019), which aligns with the delay seen in this study in the Spanish Eurosiberian region. On the other hand, the advancement of the end of the season could be associated with the previously described advancement of the start. Similar patterns are observed in the mid-season date, with advancements between 1 and 2 days across Spain except in Galicia, corresponding with the shortening of the vegetative growth season detected by Oteros *et al.* (2015).

Some regional results and differential behaviors by land covers present notable interest. For example, the high variability between the end and start dates of the season in farming areas could be due to various anthropogenic factors such as crop change or rotation, land use changes, or even decisions on changing sowing and harvesting dates (Oteros *et al.*, 2015; Van Oort *et al.*, 2012). These phenological changes in cultivated areas can have notable economic impacts, as the advancement of phenophases could increase crops' exposure to extreme weather events (such as late frosts), modify production, and even favor the relocation of crops due to changes in areas traditionally suitable for cultivation (Chmielewski *et al.*, 2004; Oteros *et al.*, 2015).

In addition to the highlighted phenological changes, one of the most important results of this study is the increase in NDVI (the initial and final values of the season, the maximum value, and the base value) throughout the entire time series in practically all of Spain and in all covers. The increasing photosynthetic activity aligns with other studies that have used time series of satellite images on a global scale and have documented a generalized greening in recent decades in response to climate changes

(Nemani *et al.*, 2003; Zhu *et al.*, 2013). At the national level, during the period 1982-1999, Alcaraz-Segura *et al.* (2010) also recorded positive NDVI trends, while Gutiérrez Hernández (2022) between 2000 and 2020 and Novillo *et al.* (2019) between 2001 and 2016 observed a positive trend across the peninsula except in the Atlantic region, where the trend was negative (Vicente-Serrano *et al.*, 2020). In the present work, an increase in the maximum NDVI value was observed in 70% of Spain, with decreases in the index value being practically irrelevant. The factors behind this change can be diverse, among which would be the generalized increase in temperature (favoring photosynthesis and plant activity (Lieth, 1974)) and changes in land management characterized by the intensification of some areas (e.g., through the creation of irrigated areas) (Stellmes *et al.*, 2013) and the extensification of others (e.g., due to the abandonment of traditional economic activities such as mountain agriculture and grazing) (Batllori and Gutiérrez, 2008). While this is true, small areas in the south of Spain and the center have shown a decrease in NDVI values. Many of them correspond with rainfed areas, where water availability has a greater impact on NDVI than temperature. This is corroborated by different studies showing that despite the notable increase in temperature on the Iberian Peninsula (del Río *et al.*, 2012; del Río *et al.*, 2011; Khorchani *et al.*, 2018), droughts have also increased, mostly associated with the decrease in precipitation and the increase in evaporative demand of the air (Vicente-Serrano *et al.*, 2017).

Finally, the results obtained in the study have shown two different behaviors between the phenophases of the Mediterranean biogeographic region, which begins the season during the rainy season (autumn) and ends it in the warmer season; and the Eurosiberian and the interior Mediterranean mountain regions, which present similar behavior as they start their season at the end of winter and end it at the end of autumn. While the variability in some phenometrics seems to have a biogeographic distribution, there is internal variability derived from the behavior of different covers, for example, there may exist in the same region covers with both advancement and delay of the start and end dates of the season. This has been seen in different studies developed both at the national (Caparros-Santiago and Rodríguez-Galiano, 2020; Novillo *et al.*, 2019) and European level (Menzel *et al.*, 2006).

This work, focused on the description of phenological characteristics and changes observed in recent decades, constitutes a first stage that opens up new and interesting lines of future research. The results shown here can be the start of other studies that seek to explain both the variability and the observed phenological changes based on the relationship of the phenometrics with changes in land management and climate observed in Spain, both at the national and regional levels.

Acknowledgements

This study was funded by the projects PTED2021-129152B-C41, PID2022-137244OB-I00, supported by the Spanish Ministry of Science and the European Regional Development Fund (FEDER), project 2857/2022 funded by the Spanish National Parks Agency, the MEHYDRO project (LINKB20080) supported by the CSIC's i-LINK 2021 program, and the CROSSDRO project, funded by the AXIS program of the JPI-Climate, co-financed by the European Commission.

References

Ahas, R., Aasa, A., Menzel, A., Fedotova, V. G., & Scheifinger, H. 2002. Changes in European spring phenology. *International Journal of Climatology*, *22*(14), 1727-1738. https://doi.org/10.1002/joc.818

Alcaraz Segura, D. 2006. Caracterización del funcionamiento de los ecosistemas ibéricos mediante teledetección. *Ecosistemas*, 15, 113–117.

Alcaraz-Segura, D., Cabello, J., & Paruelo, J. 2009. Baseline characterization of major Iberian vegetation types based on the NDVI dynamics. *Plant Ecology,* 202, 13–29. https://doi.org/10.1007/s11258-008-9555-2

Alcaraz-Segura, D., Liras, E., Tabik, S., Paruelo, J., & Cabello, J. 2010. Evaluating the Consistency of the 1982–1999 NDVI Trends in the Iberian Peninsula across Four Time-series Derived from the AVHRR Sensor: LTDR, GIMMS, FASIR, and PAL-II. *Sensors*, *10*(2), 1291-1314. https://doi.org/10.3390/s100201291

Amorós-López, J., Gómez-Chova, L., Alonso, L., Guanter, L., Zurita-Milla, R., Moreno, J., & Camps-Valls, G. 2013. Multitemporal fusion of Landsat/TM and ENVISAT/MERIS for crop monitoring. *International Journal of Applied Earth Observation and Geoinformation*, *23*, 132-141. https://doi.org/10.1016/j.jag.2012.12.004

Badeck, F., Bondeau, A., Böttcher, K., Doktor, D., Lucht, W., Schaber, J., & Sitch, S. 2004. Responses of spring phenology to climate change. *New Phytologist*, *162*(2), 295-309. https://doi.org/10.1111/j.1469-8137.2004.01059.x

Batllori, E., & Gutiérrez, E. 2008. Regional tree line dynamics in response to global change in the Pyrenees. *Journal of Ecology*, *96*(6), 1275-1288. https://doi.org/10.1111/j.1365-2745.2008.01429.x

Bertin, R. I. 2008. Plant Phenology And Distribution In Relation To Recent Climate Change. *The Journal of the Torrey Botanical Society*, *135*(1), 126-146. https://doi.org/10.3159/07-RP-035R.1

Caparros-Santiago, J. A., & Rodríguez-Galiano, V. F. 2020. Estimación de la fenología de la vegetación a partir de imágenes de satélite: El caso de la península ibérica e islas Baleares (2001-2017). *Revista de Teledetección*, *57*, 25. https://doi.org/10.4995/raet.2020.13632

Chmielewski, F.-M., Müller, A., & Bruns, E. 2004. Climate changes and trends in phenology of fruit trees and field crops in Germany, 1961–2000. *Agricultural and Forest Meteorology*, *121*(1-2), 69-78. https://doi.org/10.1016/S0168-1923(03)00161-8

Cleland, E., Chuine, I., Menzel, A., Mooney, H., & Schwartz, M. 2007. Shifting plant phenology in response to global change. *Trends in Ecology & Evolution*, *22*(7), 357-365. https://doi.org/10.1016/j.tree.2007.04.003

Cleland, E. E., Allen, J. M., Crimmins, T. M., Dunne, J. A., Pau, S., Travers, S. E., Zavaleta, E. S., & Wolkovich, E. M. 2012. Phenological tracking enables positive species responses to climate change. *Ecology*, *93*(8), 1765-1771. https://doi.org/10.1890/11-1912.1

De Beurs, K. M., & Henebry, G. M. 2005. Land surface phenology and temperature variation in the International Geosphere-Biosphere Program high-latitude transects. *Global Change Biology*, *11*(5), 779-790. https://doi.org/10.1111/j.1365-2486.2005.00949.x

del Río, S., Herrero, L., Pinto-Gomes, C., & Penas, A. 2011. Spatial analysis of mean temperature trends in Spain over the period 1961–2006. *Global and Planetary Change*, *78*(1-2), 65-75. https://doi.org/10.1016/j.gloplacha.2011.05.012

del Río, S., Cano-Ortiz, A., Herrero, L., & Penas, A. 2012. Recent trends in mean maximum and minimum air temperatures over Spain (1961–2006). *Theoretical and Applied Climatology*, *109*(3-4), 605-626. https://doi.org/10.1007/s00704-012-0593-2

Díaz-Delgado, R., Lloret, F., Pons, X., & Terradas, J. 2002. Satellite evidence of decreasing resilience in mediterranean plant communities after recurrent wildfires. *Ecology*, *83*(8), 2293-2303. https://doi.org/10.1890/0012-9658(2002)083[2293:SEODRI]2.0.CO;2

Eastman, J. R., Sangermano, F., Machado, E. A., Rogan, J., & Anyamba, A. 2013. Global trends in seasonality of Normalized Difference Vegetation Index (NDVI), 1982-2011. *Remote Sensing*, 5(10), 4799–4818. https://doi.org/10.3390/rs5104799

Eklundh, L., & Jönsson, P. 2015. TIMESAT: A Software Package for Time-Series Processing and Assessment of Vegetation Dynamics. En C. Kuenzer, S. Dech, & W. Wagner (Eds.), *Remote Sensing Time Series* (Vol. 22, pp. 141-158). Springer International Publishing. https://doi.org/10.1007/978-3-319-15967-6_7

Eklundh, L., & Jönsson, P. 2017. TIMESAT 3.3 with seasonal trend decomposition and parallel processing Software Manual. Sweden: Lund and Malmo University.

Fernandes, R., & G. Leblanc, S. 2005. Parametric (modified least squares) and non-parametric (Theil–Sen) linear regressions for predicting biophysical parameters in the presence of measurement errors. *Remote Sensing of Environment*, *95*(3), 303-316. https://doi.org/10.1016/j.rse.2005.01.005

Fisher, J., Mustard, J., & Vadeboncoeur, M. 2006. Green leaf phenology at Landsat resolution: Scaling from the field to the satellite. *Remote Sensing of Environment*, *100*(2), 265-279. https://doi.org/10.1016/j.rse.2005.10.022

Fu, Y. H., Piao, S., Op de Beeck, M., Cong, N., Zhao, H., Zhang, Y., Menzel, A., & Janssens, I. A. 2014. Recent spring phenology shifts in western Central Europe based on multiscale observations: Multiscale observation of spring phenology. *Global Ecology and Biogeography*, *23*(11), 1255-1263. https://doi.org/10.1111/geb.12210

García-Mozo, H., Mestre, A., & Galán, C. 2010. Phenological trends in southern Spain: A response to climate change. *Agricultural and Forest Meteorology*, *150*(4), 575-580. https://doi.org/10.1016/j.agrformet.2010.01.023

Ge, Q., Wang, H., Rutishauser, T., & Dai, J. 2015. Phenological response to climate change in China: A meta-analysis. *Global Change Biology*, *21*(1), 265-274. https://doi.org/10.1111/gcb.12648

Gill, A. L., Gallinat, A. S., Sanders-DeMott, R., Rigden, A. J., Short Gianotti, D. J., Mantooth, J. A., & Templer, P. H. 2015. Changes in autumn senescence in northern hemisphere deciduous trees: A meta-analysis of autumn phenology studies. *Annals of Botany*, *116*(6), 875-888. https://doi.org/10.1093/aob/mcv055

Gordo, O., & Sanz, J. J. 2009. Long-term temporal changes of plant phenology in the Western Mediterranean. *Global Change Biology*, *15*(8), 1930-1948. https://doi.org/10.1111/j.1365-2486.2009.01851.x

Gutiérrez-Hernández, O. 2020. Fenología de los ecosistemas de alta montaña en Andalucía: Análisis de la tendencia estacional del SAVI (2000-2019). *Pirineos*, 175, e055. https://doi.org/https://doi.org/10.3989/pirineos.2020.175005

Gutiérrez Hernández, O. 2022. Tendencias recientes del NDVI en Andalucía: los límites del reverdecimiento. *Boletín de La Asociación de Geógrafos Españoles, 94. https://doi.org/10.21138/bage.3246*

Helman, D. 2018. Land surface phenology: What do we really 'see' from space? *Science of the Total Environment*, 618, 665–673. https://doi.org/10.1016/j.scitotenv.2017.07.237

Jato, V., Rodríguez-Rajo, F., Méndez, J. *et al.* 2002. Phenological behaviour of Quercus in Ourense (NW Spain) and its relationship with the atmospheric pollen season. *International Journal of Biometeorology*, *46*(4), 176-184. https://doi.org/10.1007/s00484-002-0132-4

Jeong, S.-J., Ho, C.-H., Gim, H.-J., & Brown, M. E. 2011. Phenology shifts at start vs. end of growing season in temperate vegetation over the Northern Hemisphere for the period 1982-2008: PHENOLOGY SHIFTS AT START VS. END OF GROWING SEASON. *Global Change Biology*, *17*(7), 2385-2399. https://doi.org/10.1111/j.1365-2486.2011.02397.x

Jeong, S.-J., Schimel, D., Frankenberg, C., Drewry, D. T., Fisher, J. B., Verma, M., Berry, J. A., Lee, J.-E., & Joiner, J. 2017. Application of satellite solar-induced chlorophyll fluorescence to understanding large-scale variations in vegetation phenology and function over northern high latitude forests. Remote Sensing of Environment, 190, 178-187. https://doi.org/10.1016/j.rse.2016.11.021

Jönsson, P., & Eklundh, L. 2002. Seasonality extraction by function fitting to time-series of satellite sensor data. *IEEE Transactions on Geoscience and Remote Sensing*, *40*(8), 1824-1832. https://doi.org/10.1109/TGRS.2002.802519

Jönsson, P., & Eklundh, L. 2004. TIMESAT—a program for analyzing time-series of satellite sensor data. *Computers & Geosciences*, *30*(8), 833-845. https://doi.org/10.1016/j.cageo.2004.05.006

Karkauskaite, P., Tagesson, T., & Fensholt, R. 2017. Evaluation of the Plant Phenology Index (PPI), NDVI and EVI for Start-of-Season Trend Analysis of the Northern Hemisphere Boreal Zone. *Remote Sensing*, *9*(5), 485. https://doi.org/10.3390/rs9050485

Kendall, M. G. 1948. Rank correlation methods.

Kharouba, H. M., Ehrlén, J., Gelman, A., Bolmgren, K., Allen, J. M., Travers, S. E., & Wolkovich, E. M. 2018. Global shifts in the phenological synchrony of species interactions over recent decades. *Proceedings of the National Academy of Sciences*, *115*(20), 5211-5216. https://doi.org/10.1073/pnas.1714511115

Khorchani, M., Vicente-Serrano, S. M., Azorin-Molina, C., Garcia, M., Martin-Hernandez, N., Peña-Gallardo, M., El Kenawy, A., & Domínguez-Castro, F. 2018. Trends in LST over the peninsular Spain as derived from

the AVHRR imagery data. *Global and Planetary Change*, *166*, 75-93. https://doi.org/10.1016/j.gloplacha.2018.04.006

Kim, S.-R., Prasad, A. K., El-Askary, H., Lee, W.-K., Kwak, D.-A., Lee, S.-H., & Kafatos, M. 2014. Application of the Savitzky-Golay Filter to Land Cover Classification Using Temporal MODIS Vegetation Indices. *Photogrammetric Engineering & Remote Sensing*, *80*(7), 675-685. https://doi.org/10.14358/PERS.80.7.675

Kudo, G., & Ida, T. Y. 2013. Early onset of spring increases the phenological mismatch between plants and pollinators. *Ecology*, *94*(10), 2311-2320. https://doi.org/10.1890/12-2003.1

Lieth, H. 1974. Purposes of a Phenology Book. En H. Lieth (Ed.), *Phenology and Seasonality Modeling* (Vol. 8, pp. 3-19). Springer Berlin Heidelberg. https://doi.org/10.1007/978-3-642-51863-8_1

Lim, P. O., Kim, H. J., & Gil Nam, H. 2007. Leaf Senescence. *Annual Review of Plant Biology*, *58*(1), 115-136. https://doi.org/10.1146/annurev.arplant.57.032905.105316

Liu, Q., Fu, Y. H., Zeng, Z., Huang, M., Li, X., & Piao, S. 2016. Temperature, precipitation, and insolation effects on autumn vegetation phenology in temperate China. *Global Change Biology*, *22*(2), 644-655. https://doi.org/10.1111/gcb.13081

Lunetta, R. S., Knight, J. F., Ediriwickrema, J., Lyon, J. G., & Worthy, L. D. 2006. Land-cover change detection using multi-temporal MODIS NDVI data. *Remote Sensing of Environment*, *105*(2), 142-154. https://doi.org/10.1016/j.rse.2006.06.018

Mann, H. B. 1945. Nonparametric Tests Against Trend. *Econometrica*, *13*(3), 245. https://doi.org/10.2307/1907187

MAPA. 1992. Mapa de Cultivos y Aprovechamientos 1980-1990. Ministerio de Agricultura Pesca y Alimentación. Gobierno de España. https://www.mapa.gob.es/es/cartografia-y-sig/publicaciones/agricultura/mac_1980_1990.aspx

Marraccini, E., Debolini, M., Moulery, M., Abrantes, P., Bouchier, A., Chéry, J.-P., Sanz Sanz, E., Sabbatini, T., & Napoleone, C. 2015. Common features and different trajectories of land cover changes in six Western Mediterranean urban regions. *Applied Geography*, *62*, 347-356. https://doi.org/10.1016/j.apgeog.2015.05.004

Martínez, B., & Gilabert, M. A. 2009. Vegetation dynamics from NDVI time series analysis using the wavelet transform. *Remote Sensing of Environment*, *113*(9), 1823-1842. https://doi.org/10.1016/j.rse.2009.04.016

Matesanz, A. Escudero, F. Valladares. 2009. Impact of three global change drivers on a Mediterranean shrub. *Ecology*, 90 (2009), pp. 2609-2621

Menzel, A. 2002. Phenology: its importance to the global change community. *Climatic Change*, *54*(4), 379-385. https://doi.org/10.1023/A:1016125215496

Menzel, A., Sparks, T. H., Estrella, N., Koch, E., Aasa, A., Ahas, R., Alm-Kübler, K., Bissolli, P., Braslavská, O., Briede, A., Chmielewski, F. M., Crepinsek, Z., Curnel, Y., Dahl, Å., Defila, C., Donnelly, A., Filella, Y., Jatczak, K., Måge, F., … Zust, A. 2006. European phenological response to climate change matches the warming pattern: EUROPEAN PHENOLOGICAL RESPONSE TO CLIMATE CHANGE. *Global Change Biology*, *12*(10), 1969-1976. https://doi.org/10.1111/j.1365-2486.2006.01193.x

Miao, L., Müller, D., Cui, X., & Ma, M. 2017. Changes in vegetation phenology on the Mongolian Plateau and their climatic determinants. *PLOS ONE*, *12*(12), e0190313. https://doi.org/10.1371/journal.pone.0190313

MITECO. s.f. Fenología y cambio climático en la Red Española de Reservas de Biosfera. Recuperado de https://www.miteco.gob.es/es/ceneam/grupos-de-trabajo-y-seminarios/red-espanola-reservas-biosfera/fenologia-cambio-climatico-reservas-biosfera.aspx

Motohka, T., Nasahara, K. N., Oguma, H., & Tsuchida, S. 2010. Applicability of Green-Red Vegetation Index for Remote Sensing of Vegetation Phenology. *Remote Sensing*, *2*(10), 2369-2387. https://doi.org/10.3390/rs2102369

Nemani, R. R., Keeling, C. D., Hashimoto, H., Jolly, W. M., Piper, S. C., Tucker, C. J., Myneni, R. B., & Running, S. W. 2003. Climate-Driven Increases in Global Terrestrial Net Primary Production from 1982 to 1999. *Science*, *300*(5625), 1560-1563. https://doi.org/10.1126/science.1082750

Novillo, C., Arrogante-Funes, P., & Romero-Calcerrada, R. 2019. Recent NDVI Trends in Mainland Spain: Land-Cover and Phytoclimatic-Type Implications. *ISPRS International Journal of Geo-Information*, *8*(1), 43. https://doi.org/10.3390/ijgi8010043

Oteros, J., García-Mozo, H., Botey, R., Mestre, A., & Galán, C. 2015. Variations in cereal crop phenology in Spain over the last twenty-six years (1986–2012). *Climatic Change*, *130*(4), 545-558. https://doi.org/10.1007/s10584-015-1363-9

Palazón, A., Aragonés, L., & López, I. 2016. Evaluation of coastal management: Study case in the province of Alicante, Spain. *Science of The Total Environment*, *572*, 1184-1194. https://doi.org/10.1016/j.scitotenv.2016.08.032

Pastor, F., Valiente, J. A., & Khodayar, S. 2020. A Warming Mediterranean: 38 Years of Increasing Sea Surface Temperature. *Remote Sensing*, *12*(17), 2687. https://doi.org/10.3390/rs12172687

Peng, H., Wang, S., & Wang, X. 2008. Consistency and asymptotic distribution of the Theil–Sen estimator. *Journal of Statistical Planning and Inference*, *138*(6), 1836-1850. https://doi.org/10.1016/j.jspi.2007.06.036

Peñuelas, J., Filella, I., & Comas, P. (2002). Changed plant and animal life cycles from 1952 to 2000 in the Mediterranean region. *Global Change Biology*, *8*(6), 531-544.S.

Peñuelas, J., Filella, I., & Comas, P. 2002. Changed plant and animal life cycles from 1952 to 2000 in the Mediterranean region: PHENOLOGICAL EFFECTS OF CLIMATE WARMING. *Global Change Biology*, *8*(6), 531-544. https://doi.org/10.1046/j.1365-2486.2002.00489.x

Piao, S., Fang, J., Zhou, L., Ciais, P., & Zhu, B. 2006. Variations in satellite-derived phenology in China's temperate vegetation: SATELLITE-DERIVED PHENOLOGY IN CHINA. *Global Change Biology*, *12*(4), 672-685. https://doi.org/10.1111/j.1365-2486.2006.01123.x

Piao, S., Liu, Q., Chen, A., Janssens, I. A., Fu, Y., Dai, J., Liu, L., Lian, X., Shen, M., & Zhu, X. 2019. Plant phenology and global climate change: Current progresses and challenges. *Global Change Biology*, *25*(6), 1922-1940. https://doi.org/10.1111/gcb.14619

Prieto, F., RUIZ, P., & Martínez, J. (2008). Prospectiva 2030 en los cambios de ocupación del suelo en España y sus impactos en el ciclo hidrológico. In *VI Congreso Ibérico sobre Gestión y Planificación del Agua. Fundación Nueva Cultura del Agua* (pp. 4-7).

Prislan, P., Gričar, J., Čufar, K., de Luis, M., Merela, M., & Rossi, S. 2019. Growing season and radial growth predicted for Fagus sylvatica under climate change. *Climatic Change*, *153*(1-2), 181-197. https://doi.org/10.1007/s10584-019-02374-0

R Core Team 2020. R: A language and environment for statistical computing. R Foundation for Statistical Computing, Vienna, Austria. URL https://www.R-project.org/

Rathcke, B., & Lacey, E. P. 1985. Phenological Patterns of Terrestrial Plants. *Annual Review of Ecology and Systematics*, *16*(1), 179-214. https://doi.org/10.1146/annurev.es.16.110185.001143

Reed, B. C. 2006. Trend Analysis of Time-Series Phenology of North America Derived from Satellite Data. *GIScience & Remote Sensing*, *43*(1), 24-38. https://doi.org/10.2747/1548-1603.43.1.24

Reed, B. C., Schwartz, M. D., & Xiao, X. 2009. Remote Sensing Phenology. En A. Noormets (Ed.), *Phenology of Ecosystem Processes* (pp. 231-246). Springer New York. https://doi.org/10.1007/978-1-4419-0026-5_10

Richardson, A. D., Keenan, T. F., Migliavacca, M., Ryu, Y., Sonnentag, O., & Toomey, M. 2013. Climate change, phenology, and phenological control of vegetation feedbacks to the climate system. *Agricultural and Forest Meteorology*, *169*, 156-173. https://doi.org/10.1016/j.agrformet.2012.09.012

Rodriguez-Galiano, V. F., Dash, J., & Atkinson, P. M. 2015. Intercomparison of satellite sensor land surface phenology and ground phenology in Europe: Inter-annual comparison and modelling. *Geophysical Research Letters*, *42*(7), 2253-2260. https://doi.org/10.1002/2015GL063586

Rossi, S., Morin, H., Deslauriers, A., & Plourde, P.-Y. 2011. Predicting xylem phenology in black spruce under climate warming: XYLEM PHENOLOGY UNDER CLIMATE WARMING. *Global Change Biology*, *17*(1), 614-625. https://doi.org/10.1111/j.1365-2486.2010.02191.x

Rubio-Cuadrado, Á., Camarero, J. J., Rodríguez-Calcerrada, J., Perea, R., Gómez, C., Montes, F., & Gil, L. 2021. Impact of successive spring frosts on leaf phenology and radial growth in three deciduous tree species with contrasting climate requirements in central Spain. *Tree Physiology*, *41*(12), 2279-2292. https://doi.org/10.1093/treephys/tpab076

Sakamoto, T., Yokozawa, M., Toritani, H., Shibayama, M., Ishitsuka, N., & Ohno, H. 2005. A crop phenology detection method using time-series MODIS data. *Remote Sensing of Environment*, *96*(3-4), 366-374. https://doi.org/10.1016/j.rse.2005.03.008

Schwartz, M. D. 2013. Phenology: An Integrative Environmental Science. In M. D. Schwartz (Ed.), Phenology: An Integrative Environmental Science. *Springer Netherlands*. https://doi.org/10.1007/978-94-007-6925-0

Stagge, J. H., Tallaksen, L. M., Gudmundsson, L., Van Loon, A. F., & Stahl, K. 2015. Candidate Distributions for Climatological Drought Indices (SPI and SPEI). *International Journal of Climatology*, *35*(13), 4027-4040. https://doi.org/10.1002/joc.4267

Stellmes, M., Röder, A., Udelhoven, T., & Hill, J. 2013. Mapping syndromes of land change in Spain with remote sensing time series, demographic and climatic data. *Land Use Policy*, *30*(1), 685-702. https://doi.org/10.1016/j.landusepol.2012.05.007

Stöckli, R., & Vidale, P. L. 2004. European plant phenology and climate as seen in a 20-year AVHRR land-surface parameter dataset. *International Journal of Remote Sensing*, *25*(17), 3303-3330. https://doi.org/10.1080/01431160310001618149

Van Oort, P. A. J., Timmermans, B. G. H., & van Swaaij, A. C. P. M. 2012. Why farmers' sowing dates hardly change when temperature rises. *European Journal of Agronomy*, *40*, 102-111. https://doi.org/10.1016/j.eja.2012.02.005

Verger, A., Filella, I., Baret, F., & Peñuelas, J. 2016. Vegetation baseline phenology from kilometric global LAI satellite products. *Remote Sensing of Environment*, *178*, 1-14. https://doi.org/10.1016/j.rse.2016.02.057

Vicente-Serrano, S. M., López-Moreno, J. I., Beguería, S., Lorenzo-Lacruz, J., Azorin-Molina, C., & Morán-Tejeda, E. 2012. Accurate Computation of a Streamflow Drought Index. *Journal of Hydrologic Engineering*, *17*(2), 318-332. https://doi.org/10.1061/(ASCE)HE.1943-5584.0000433

Vicente-Serrano, S. M., Rodríguez-Camino, E., Domínguez-Castro, F., El Kenawy, A., & Azorín-Molina, C. 2017. An updated review on recent trends in observational surface atmospheric variables and their extremes over Spain. *Cuadernos de Investigación Geográfica*, *43*(1), 209-232. https://doi.org/10.18172/cig.3134

Vicente-Serrano, S. M., Martín-Hernández, N., Reig, F., Azorin-Molina, C., Zabalza, J., Beguería, S., Domínguez-Castro, F., El Kenawy, A., Peña-Gallardo, M., Noguera, I., & García, M. 2020. Vegetation greening in Spain detected from long term data (1981–2015). *International Journal of Remote Sensing*, *41*(5), 1709-1740. https://doi.org/10.1080/01431161.2019.1674460

Vrieling, A., Meroni, M., Darvishzadeh, R., Skidmore, A. K., Wang, T., Zurita-Milla, R., Oosterbeek, K., O'Connor, B., & Paganini, M. 2018. Vegetation phenology from Sentinel-2 and field cameras for a Dutch barrier island. *Remote Sensing of Environment*, *215*, 517-529. https://doi.org/10.1016/j.rse.2018.03.014

White, K., Pontius, J., & Schaberg, P. 2014. Remote sensing of spring phenology in northeastern forests: A comparison of methods, field metrics and sources of uncertainty. *Remote Sensing of Environment*, *148*, 97-107. https://doi.org/10.1016/j.rse.2014.03.017

White, M. A., De Beurs, K. M., Didan, K., Inouye, D. W., Richardson, A. D., Jensen, O. P., O'Keefe, J., Zhang, G., Nemani, R. R., Van Leeuwen, W. J. D., Brown, J. F., De Wit, A., Schaepman, M., Lin, X., Dettinger, M., Bailey, A. S., Kimball, J., Schwartz, M. D., Baldocchi, D. D., … Lauenroth, W. K. 2009. Intercomparison, interpretation, and assessment of spring phenology in North America estimated from remote sensing for 1982-2006. *Global Change Biology*, *15*(10), 2335-2359. https://doi.org/10.1111/j.1365-2486.2009.01910.x

Willmott, C. J. 1981. ON THE VALIDATION OF MODELS. *Physical Geography*, *2*(2), 184-194. https://doi.org/10.1080/02723646.1981.10642213

Wolfe, D. W., Schwartz, M. D., Lakso, A. N., Otsuki, Y., Pool, R. M., & Shaulis, N. J. 2005. Climate change and shifts in spring phenology of three horticultural woody perennials in northeastern USA. *International Journal of Biometeorology*, *49*(5), 303-309. https://doi.org/10.1007/s00484-004-0248-9

Yang, L. H., & Rudolf, V. H. W. 2010. Phenology, ontogeny and the effects of climate change on the timing of species interactions. *Ecology Letters*, *13*(1), 1-10. https://doi.org/10.1111/j.1461-0248.2009.01402.x

Zhang, X., Friedl, M. A., Schaaf, C. B., Strahler, A. H., Hodges, J. C. F., Gao, F., Reed, B. C., & Huete, A. 2003. Monitoring vegetation phenology using MODIS. *Remote Sensing of Environment*, *84*(3), 471-475. https://doi.org/10.1016/S0034-4257(02)00135-9

Zhang, X., Wang, J., Gao, F., Liu, Y., Schaaf, C., Friedl, M., Yu, Y., Jayavelu, S., Gray, J., Liu, L., Yan, D., & Henebry, G. M. 2017. Exploration of scaling effects on coarse resolution land surface phenology. *Remote Sensing of Environment*, *190*, 318-330. https://doi.org/10.1016/j.rse.2017.01.001

Zhou, L., Tucker, C. J., Kaufmann, R. K., Slayback, D., Shabanov, N. V., & Myneni, R. B. 2001. Variations in northern vegetation activity inferred from satellite data of vegetation index during 1981 to 1999. *Journal of Geophysical Research: Atmospheres*, *106*(D17), 20069-20083. https://doi.org/10.1029/2000JD000115

Zhu, Z., Bi, J., Pan, Y., Ganguly, S., Anav, A., Xu, L., Samanta, A., Piao, S., Nemani, R., & Myneni, R. 2013. Global Data Sets of Vegetation Leaf Area Index (LAI)3g and Fraction of Photosynthetically Active Radiation (FPAR)3g Derived from Global Inventory Modeling and Mapping Studies (GIMMS) Normalized Difference Vegetation Index (NDVI3g) for the Period 1981 to 2011. *Remote Sensing*, *5*(2), 927-948. https://doi.org/10.3390/rs5020927

Supplementary material

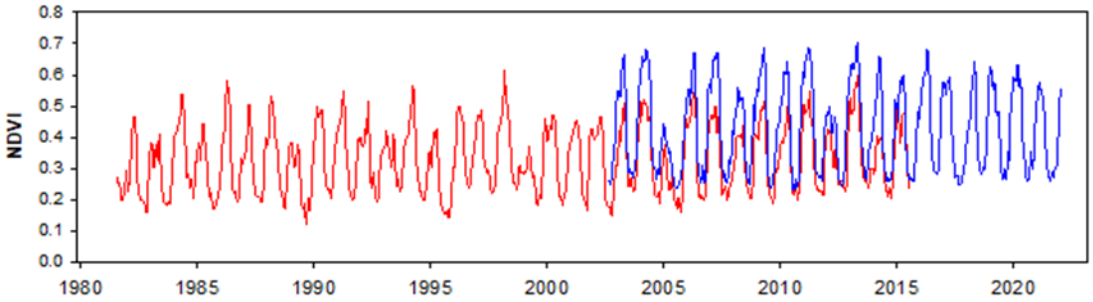

Figure S1. Evolution of the NDVI time series for a specific pixel corresponding to the series from NOAA-AVHRR satellites (red) and MODIS (blue).

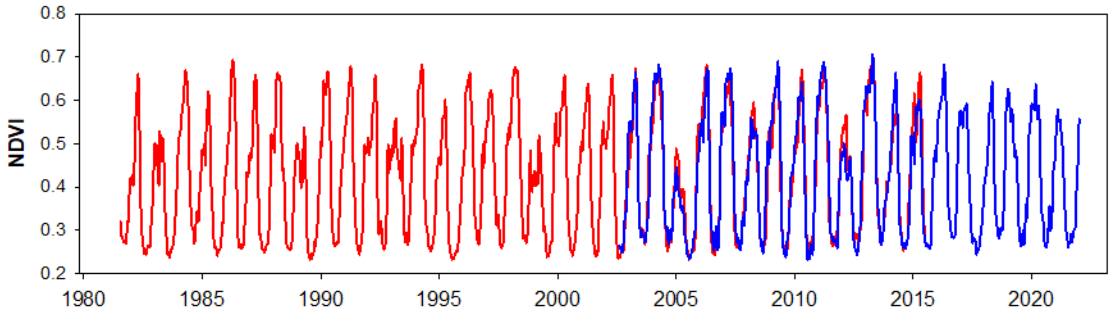

Figure S2. NDVI series from MODIS (blue) and NDVI series from NOAA-AVHRR satellites (red) merged with the MODIS series. 1982-2021.

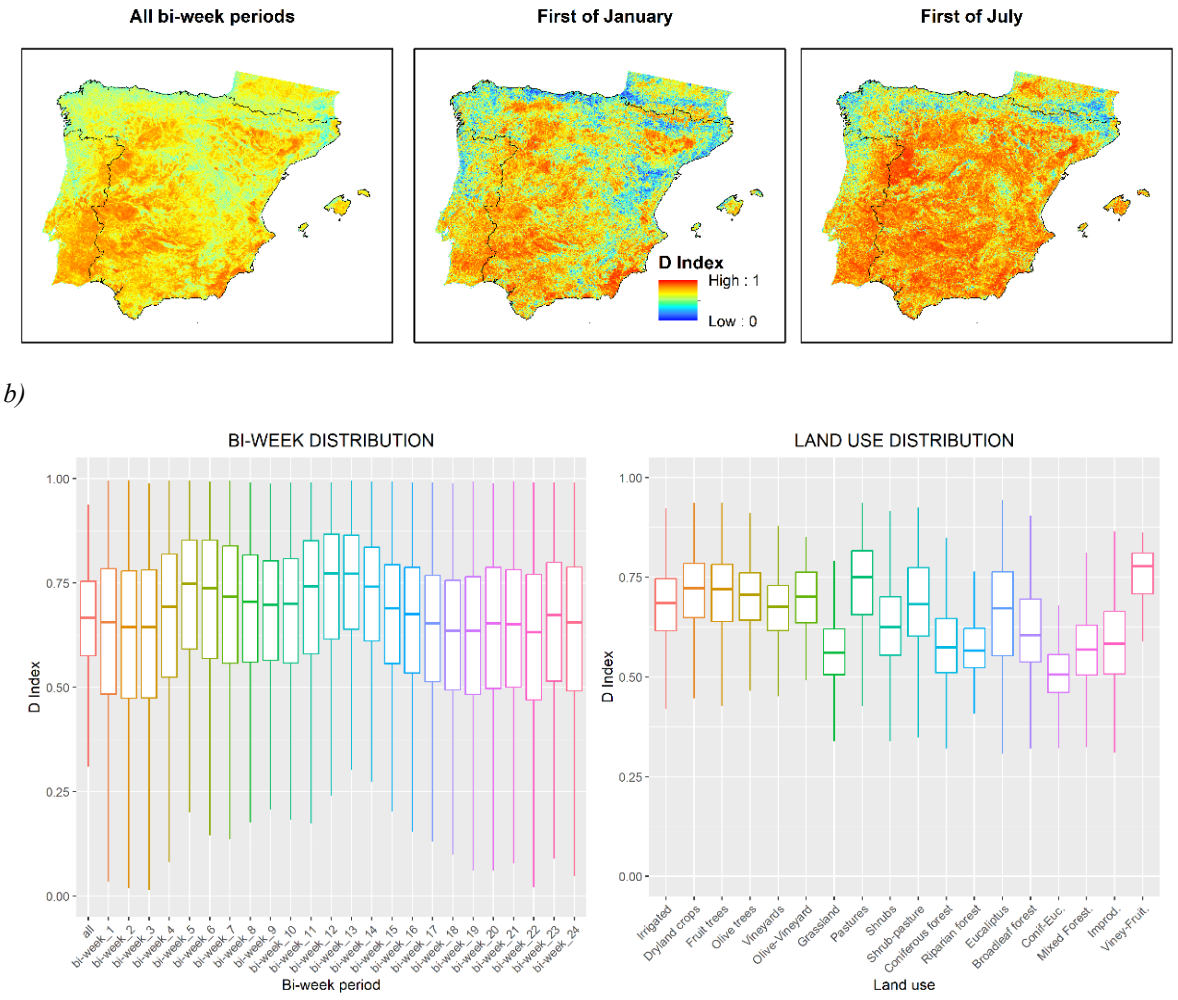

Figure S3. a) Distribution of the D index calculated for all fortnightly periods, the first in January and the first in July, b) Distribution of D index values for all weeks of the year and also by land use. 1982-2021.

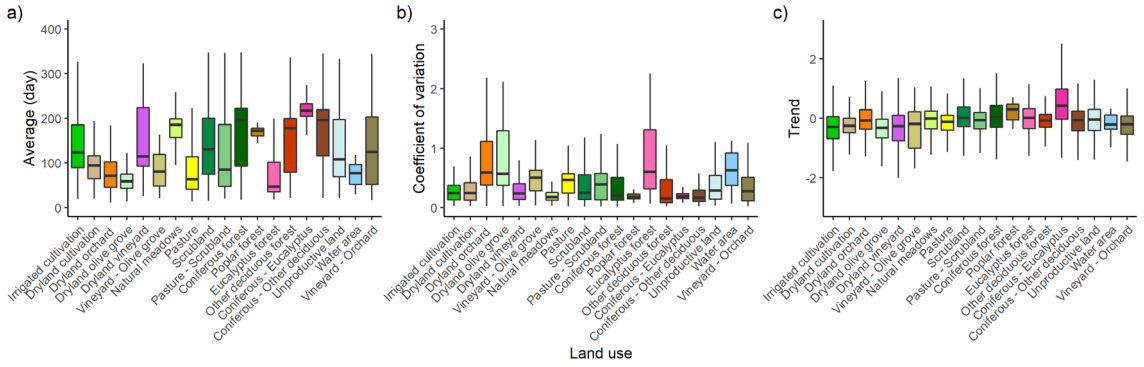

Figure S4. Mid-season date statistics throughout the series according to different types of land cover.

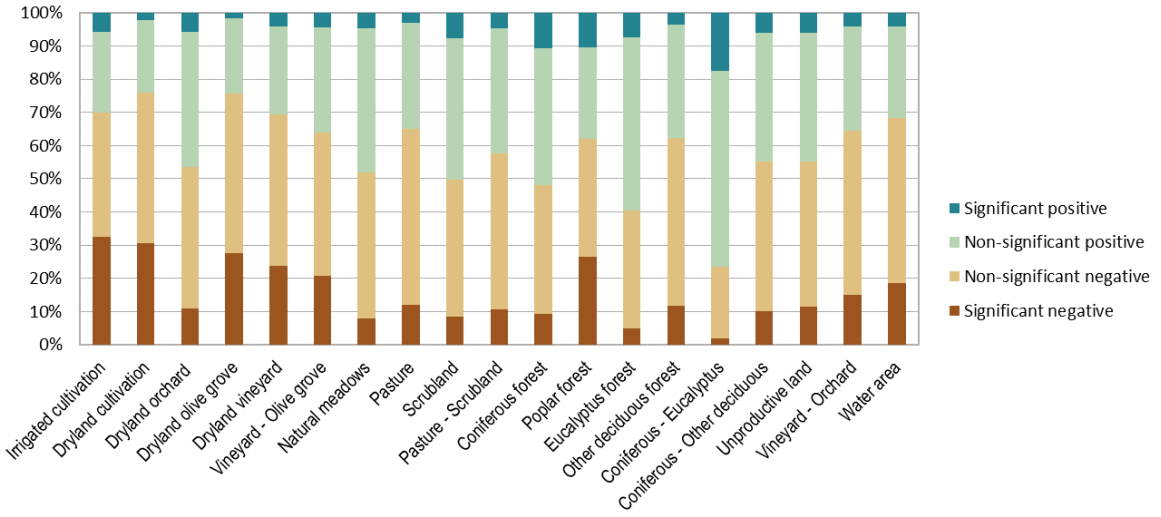

Figure S5. Changes in mid-season date by land use.

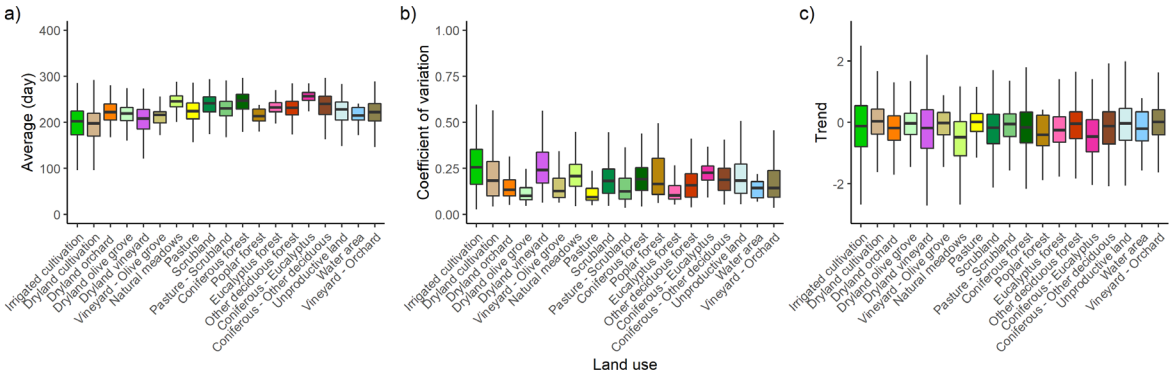

Figure S6. Season duration statistics throughout the series according to different types of land cover.

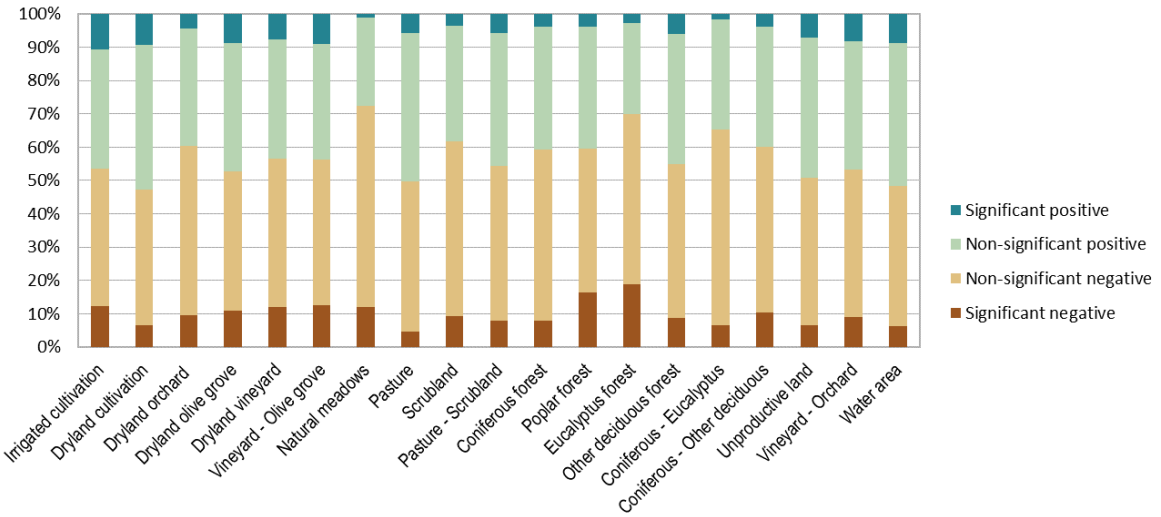

Figure S7. Changes in season duration by land use.

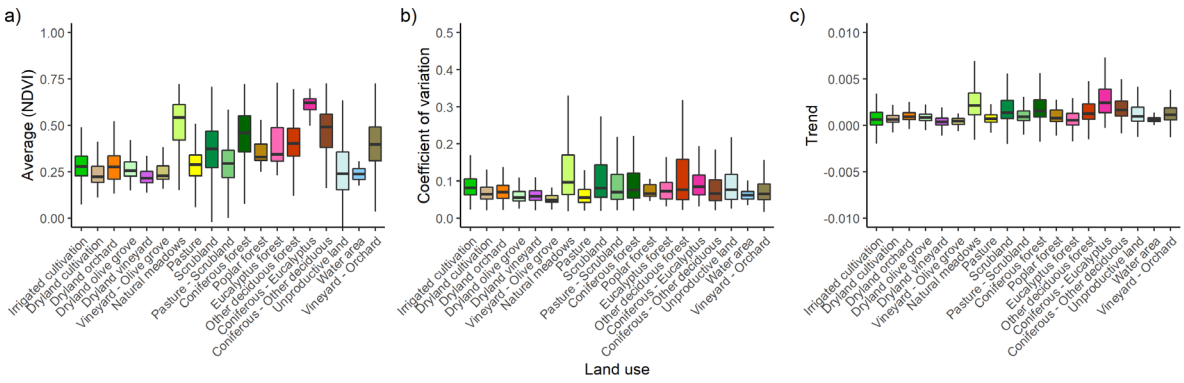

Figure S8. Base value statistics of the season throughout the series according to different types of land cover.

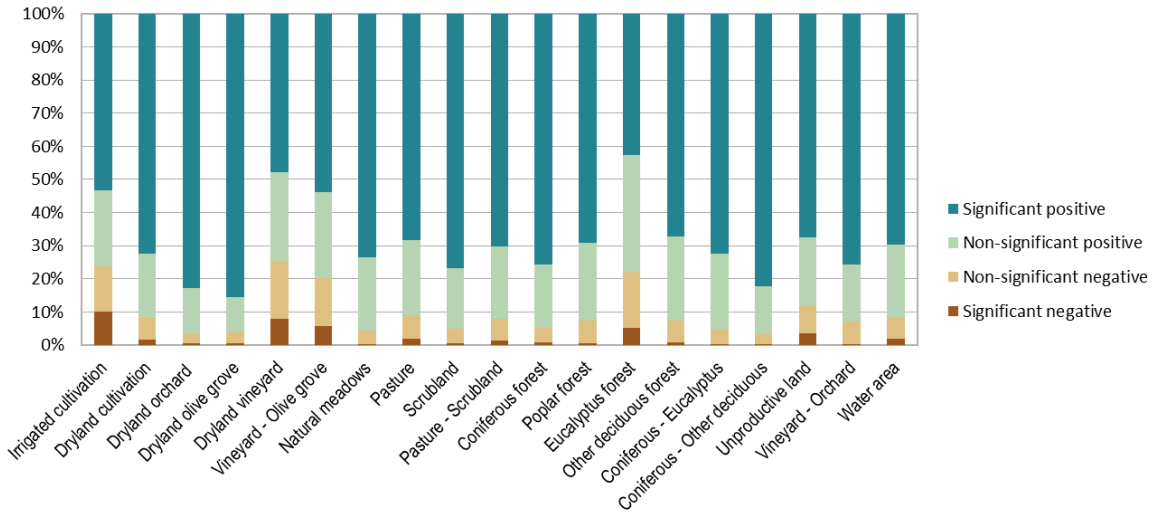

Figure S9. Changes in the base value of NDVI for the vegetative season by land use.

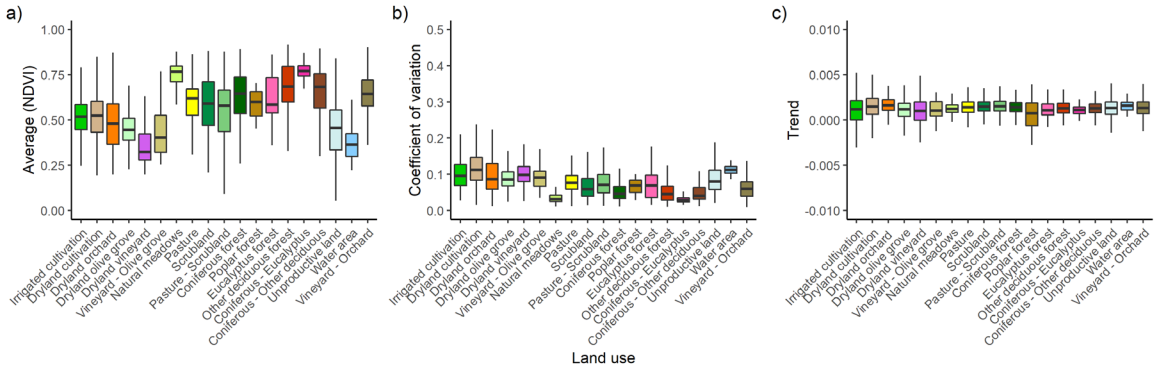

Figure S10. Maximum value statistics of the season throughout the series according to different types of land cover

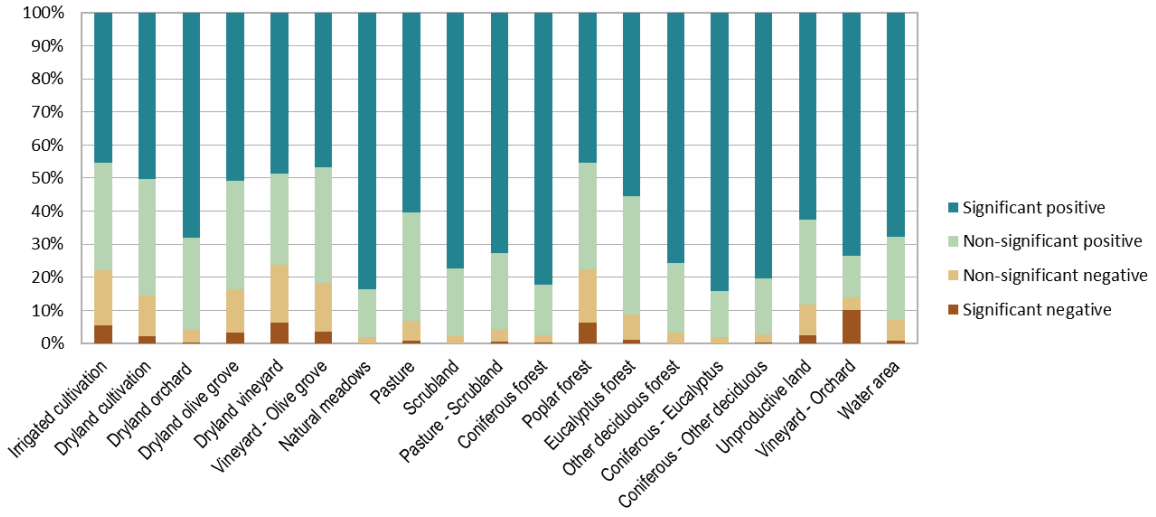

Figure S11. Changes in the maximum value of the season by land use.

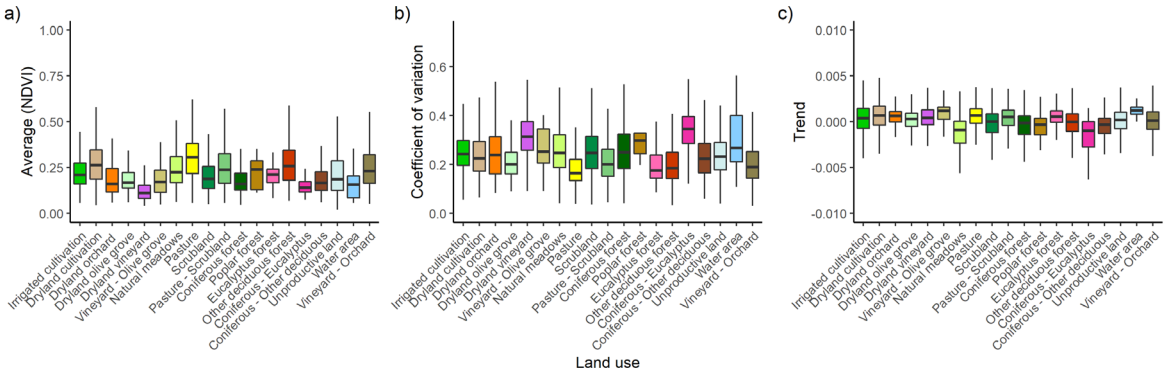

Figure S12. Season amplitude statistics throughout the series according to different types of land cover.

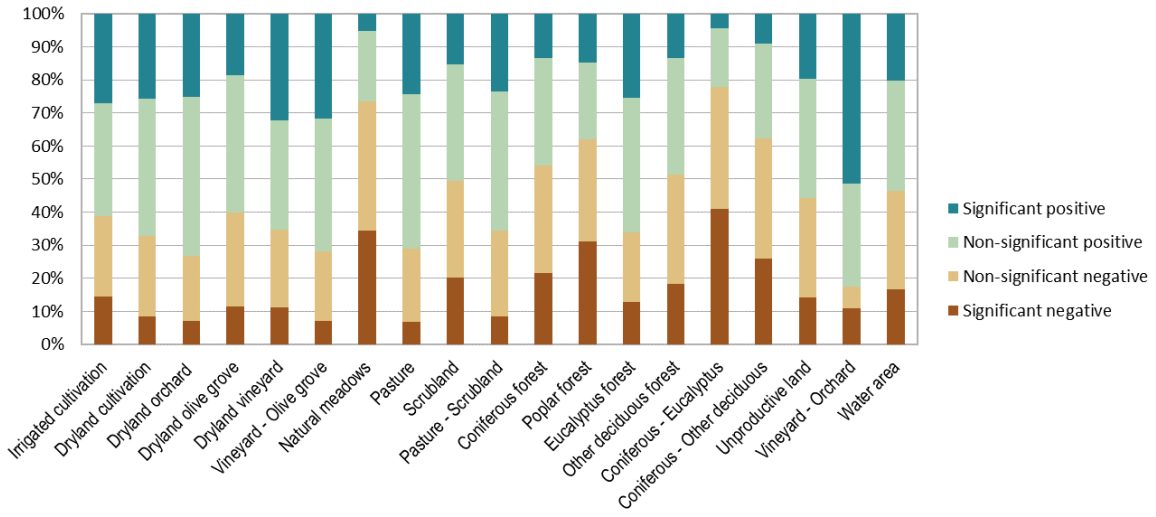

Figure S13. Changes in amplitude by land use.

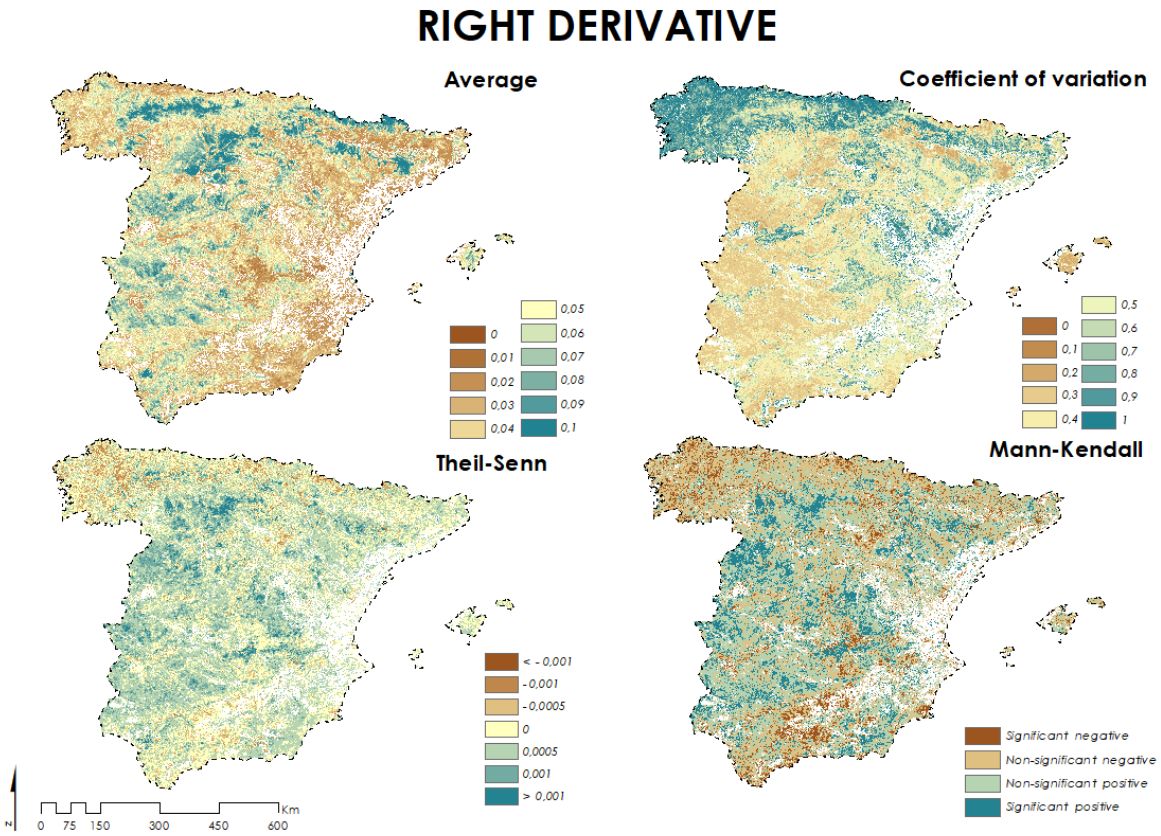

Figure S14. Maps of the statistics for the right derivative of the season.

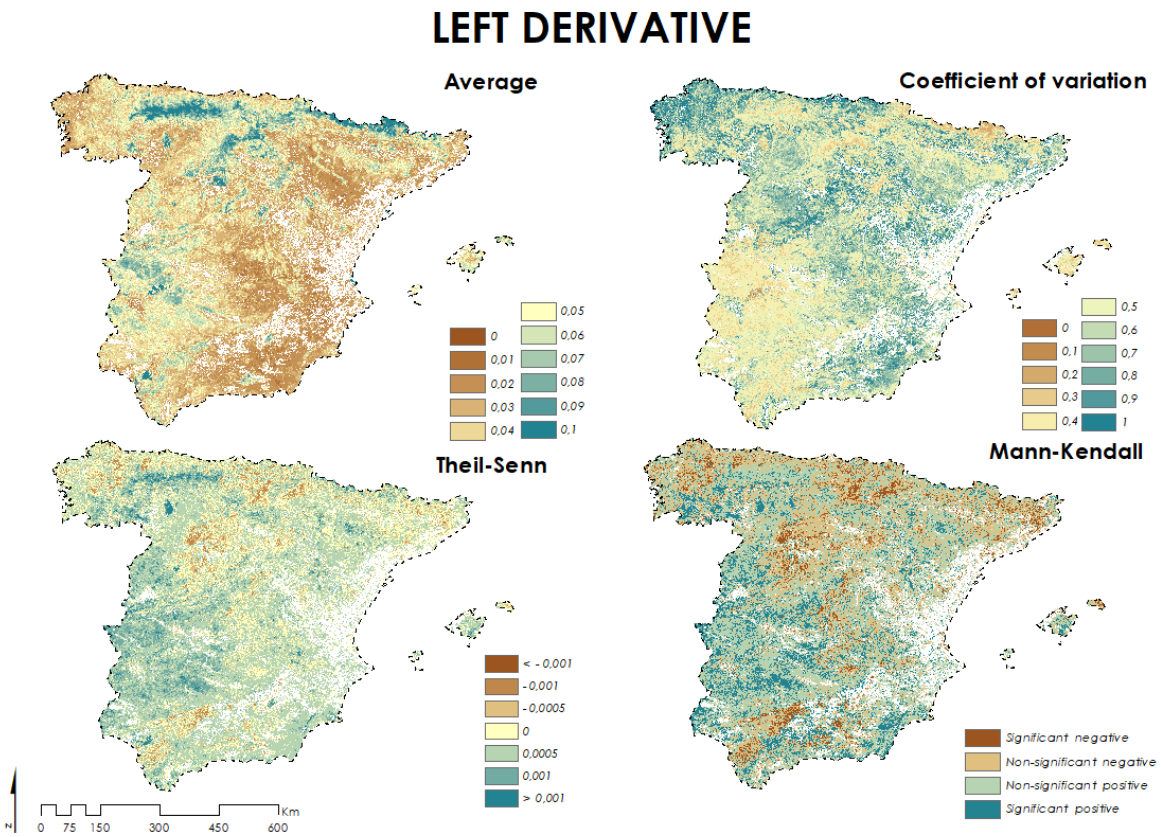

Figure S15. Maps of the statistics for the left derivative of the season

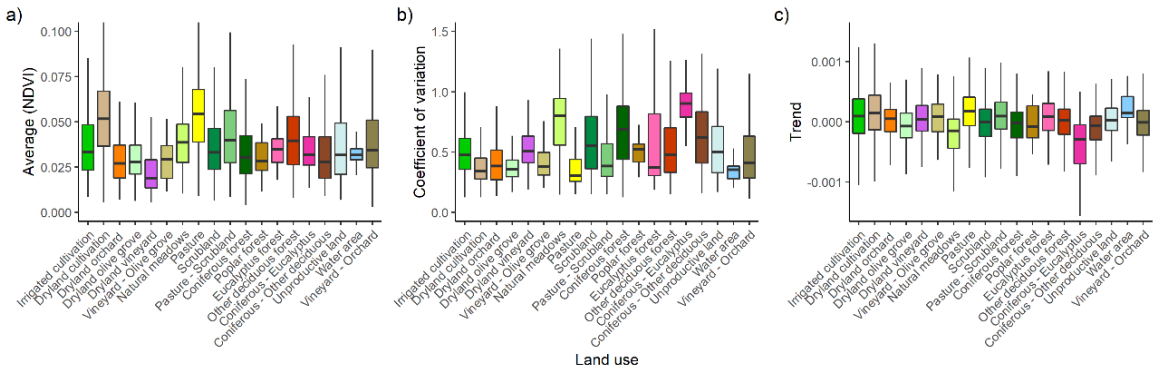

Figure S16. Right derivative statistics of the season throughout the series according to different types of land cover.

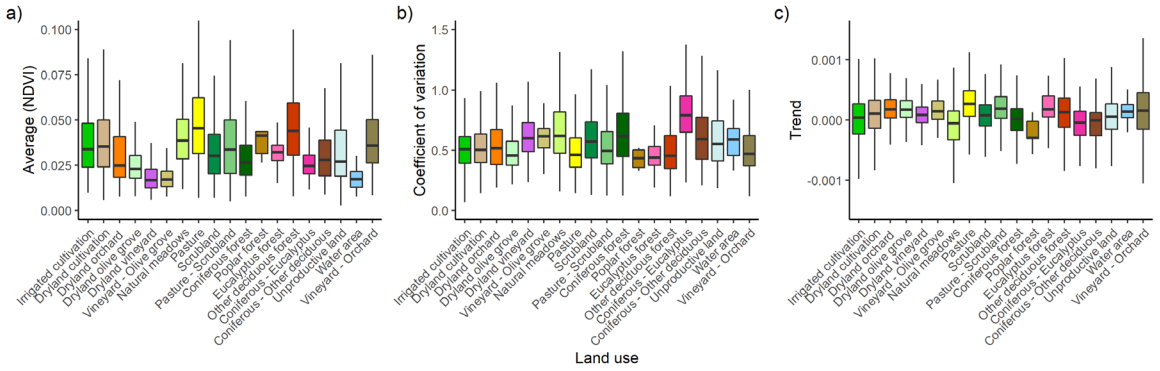

Figure S17. Left derivative statistics of the season throughout the series according to different types of land cover.

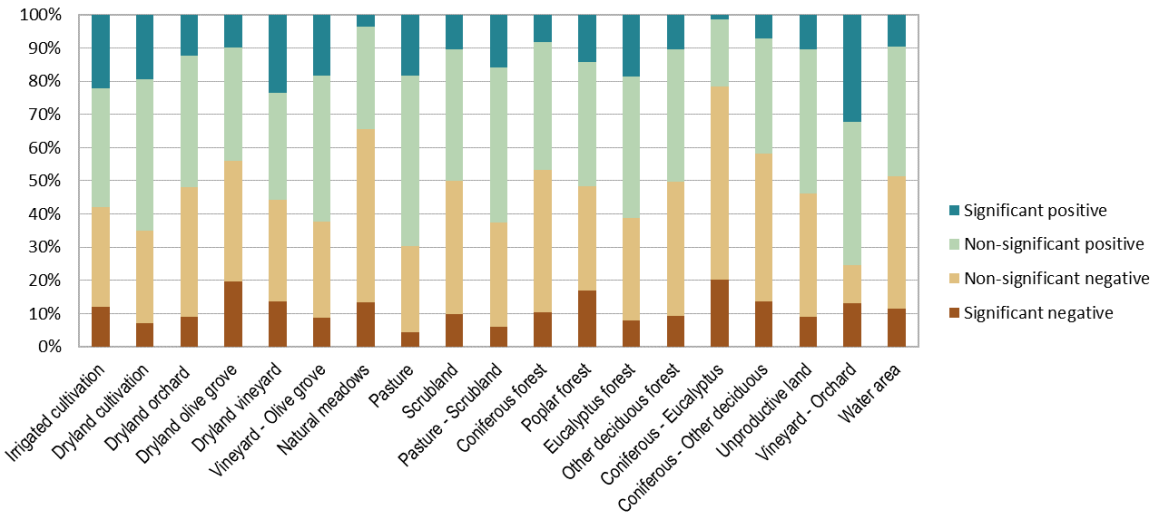

Figure S18. Changes in the right derivative by land use.

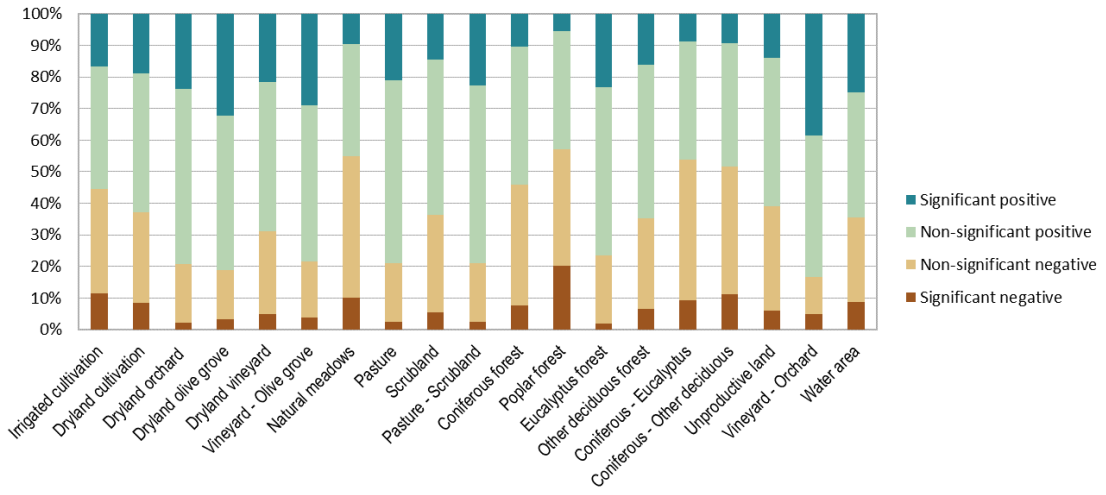

Figure S19. Changes in the left derivative by land use.

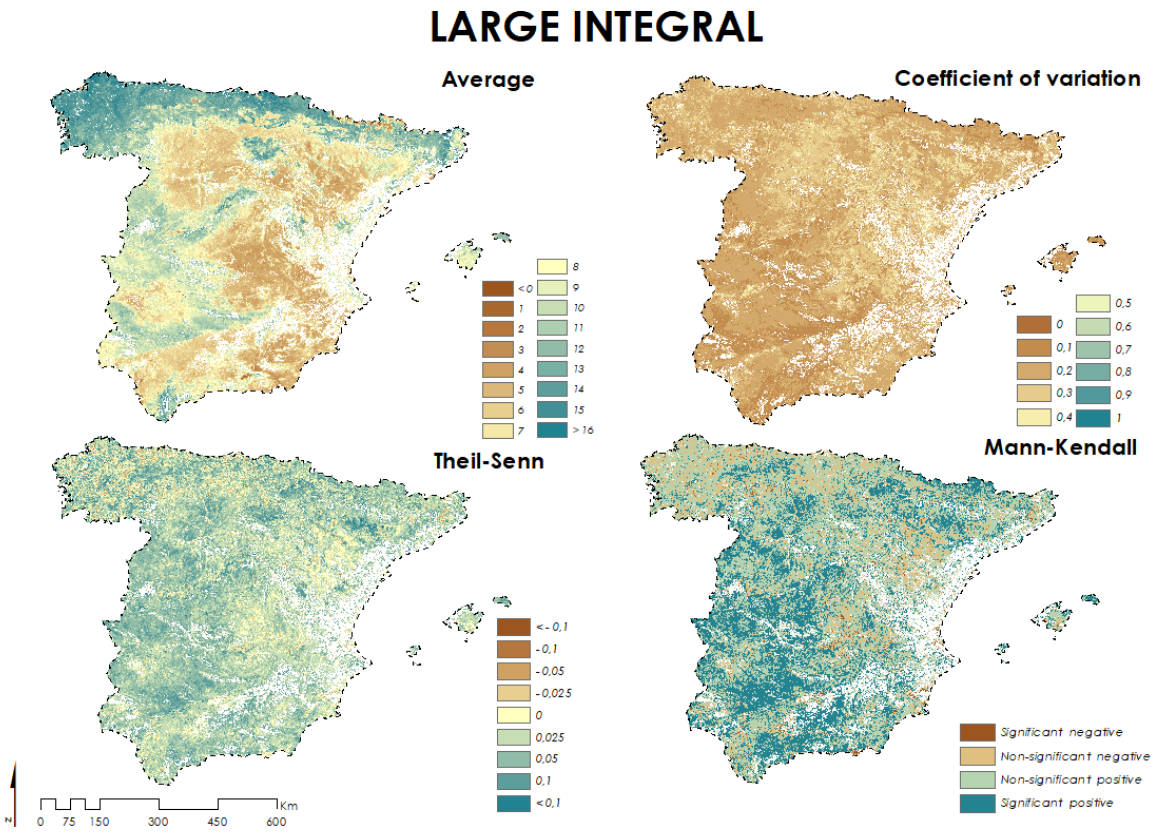

Figure S20. Maps of the statistics for the large integral of the season.

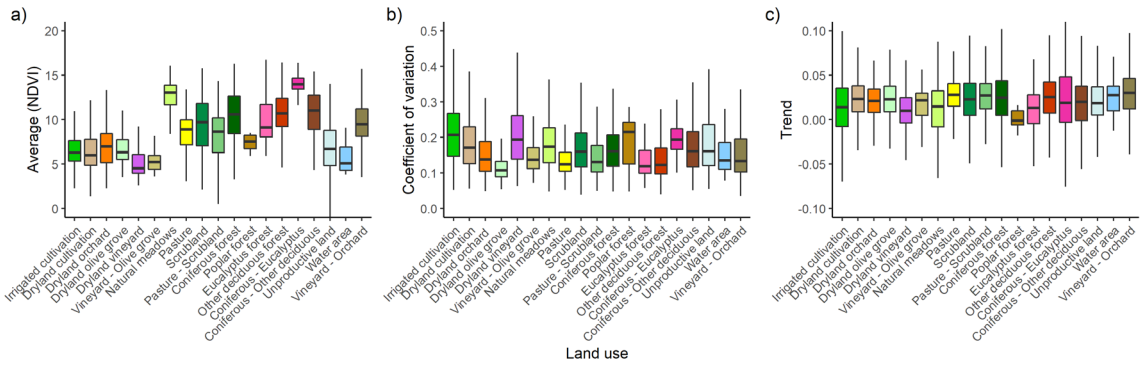

Figure S21. Large integral statistics of the season throughout the series according to different types of land cover.

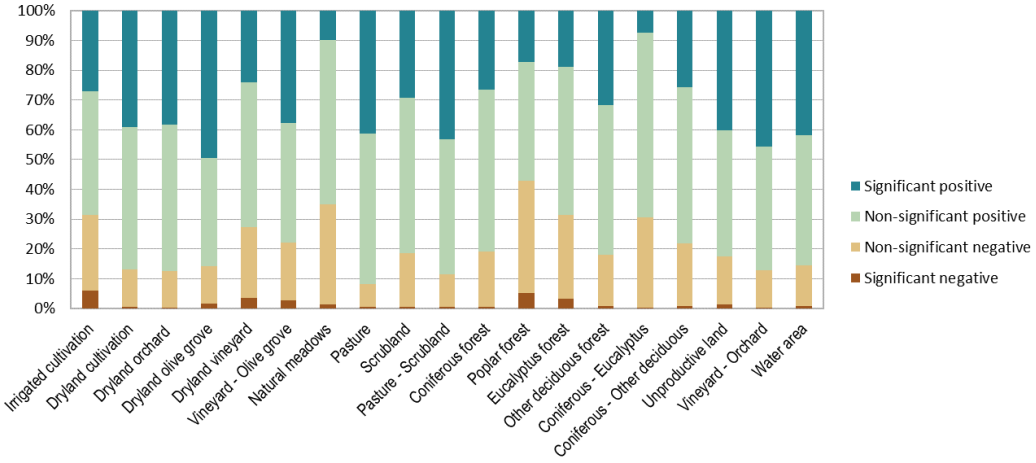

Figure S22. Changes in the large integral by land use.

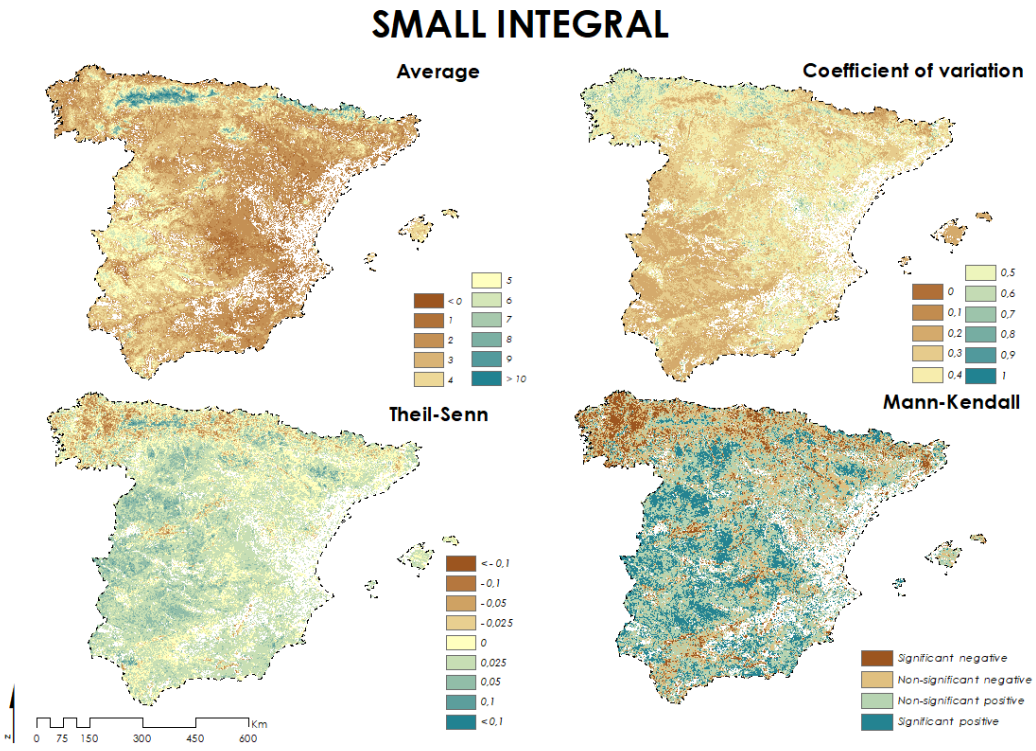

Figure S23. Maps of the statistics for the small integral of the season.

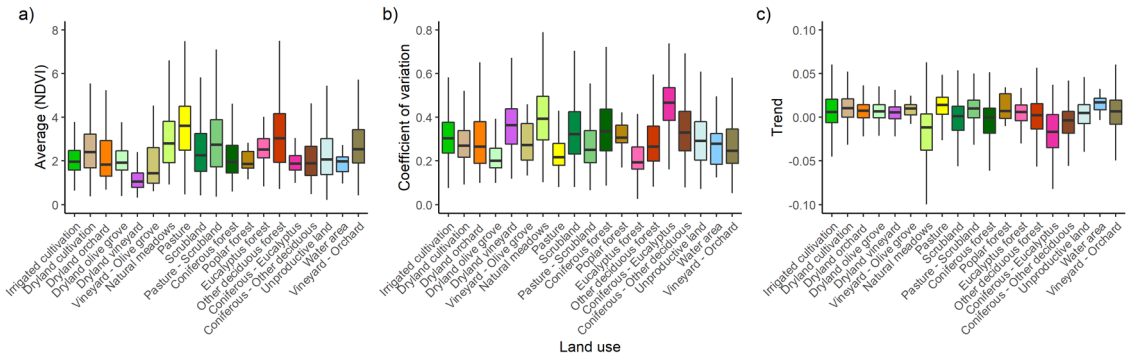

Figure S24. Small integral statistics of the season throughout the series according to different types of land cover.

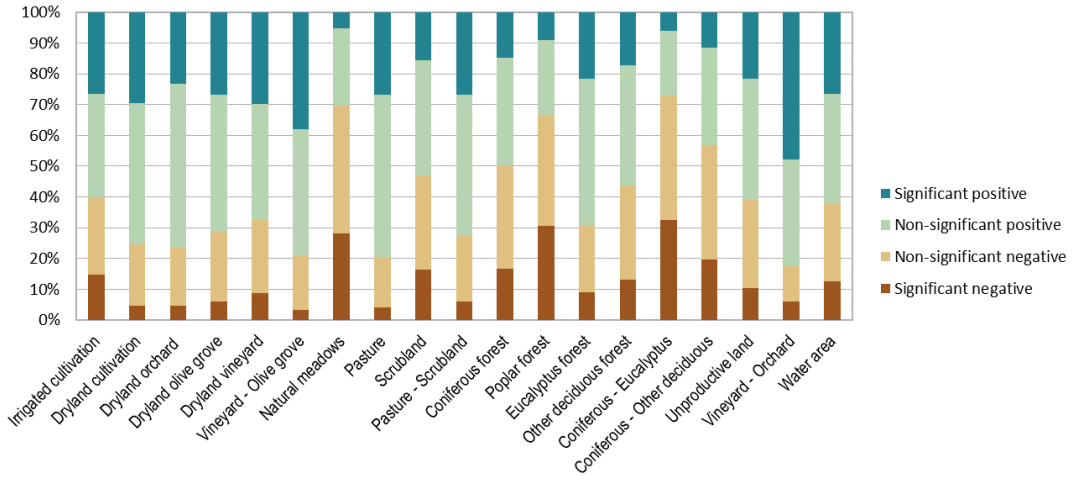

Figure S25. Changes in the small integral by land use.

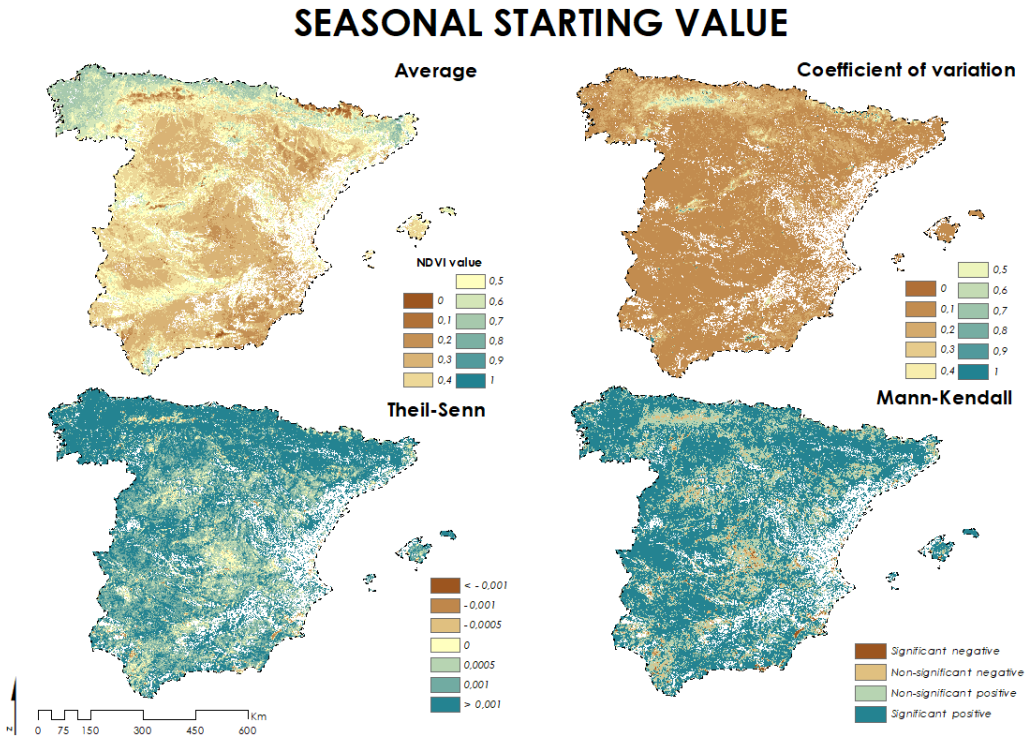

Figure S26. Maps of the statistics for the initial value of the season.

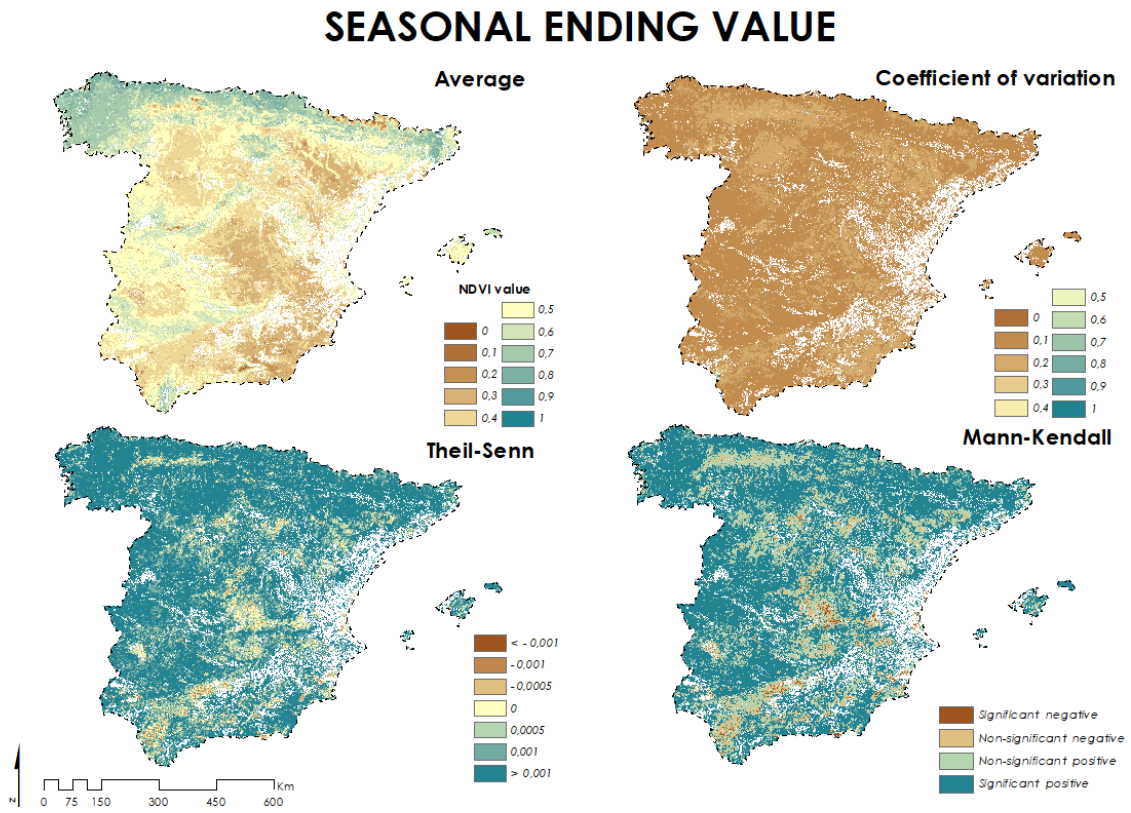

Figure S27. Maps of the statistics for the final value of the season.

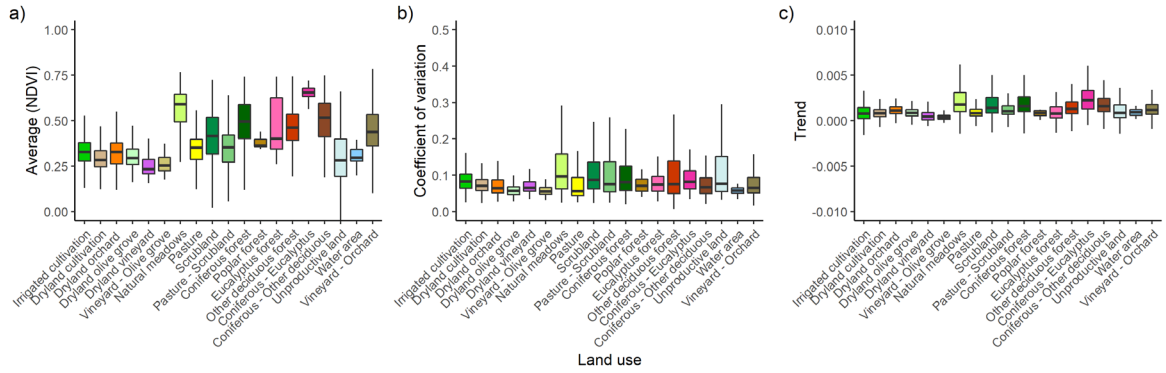

Figure S28. Start value statistics of the season throughout the series according to different types of land cover.

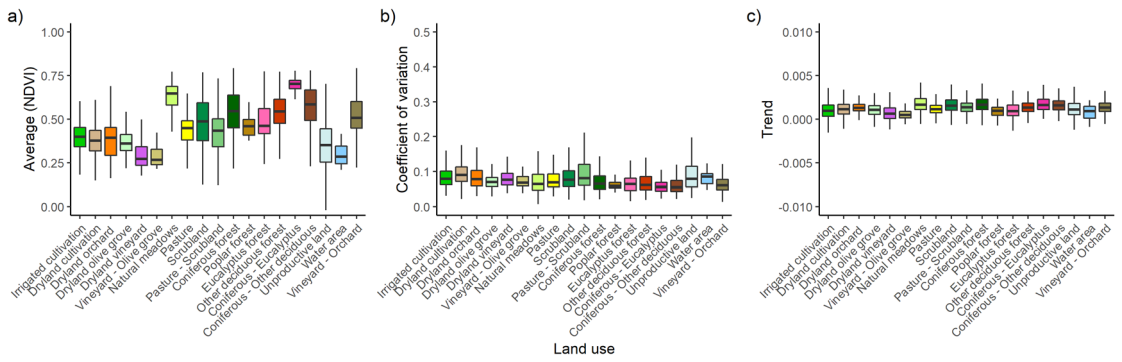

Figure S29. End value statistics of the season throughout the series according to different types of land cover.

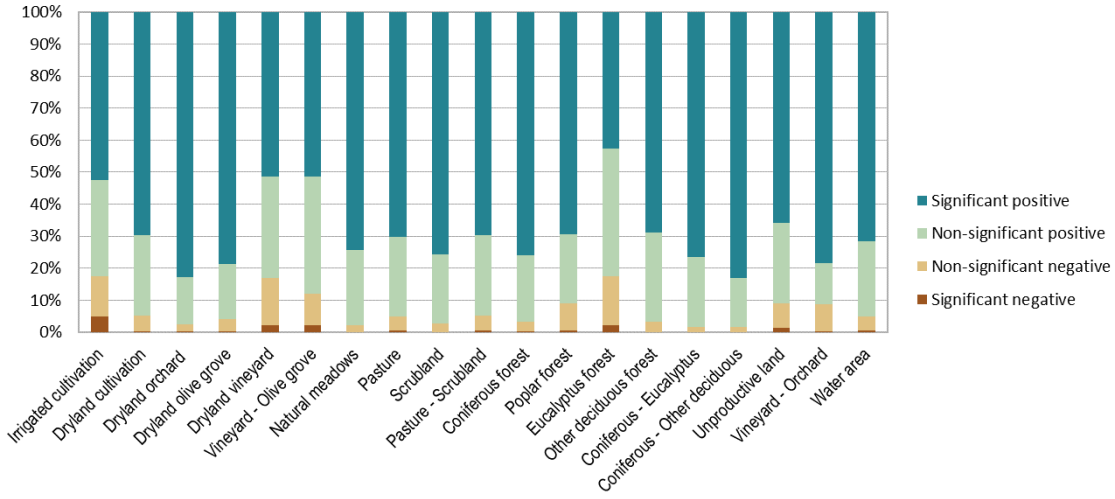

Figure S30. Changes in the start value of the season by land use.

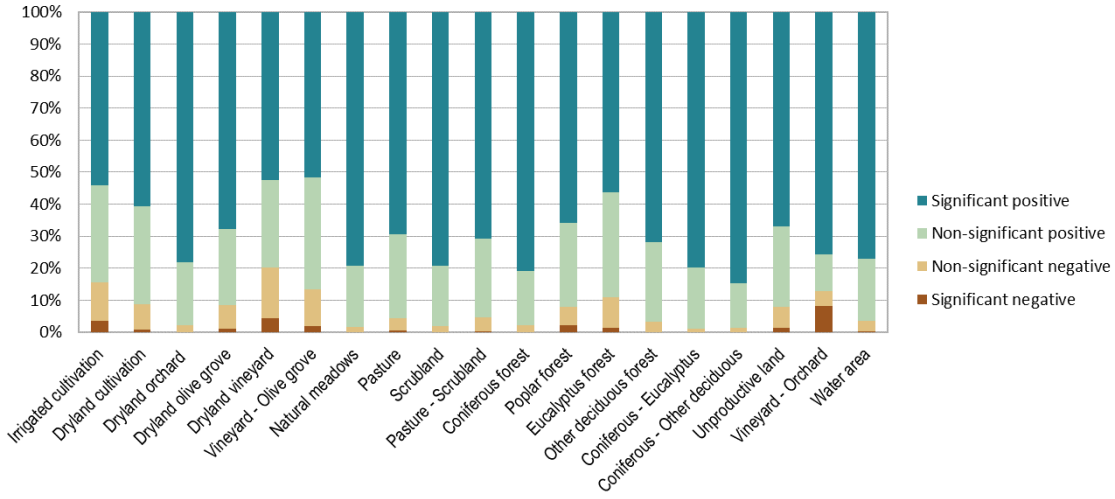

Figure S31. Changes in the end value of the season by land use.